Gandin et al, nanoCAGE reveals 5' UTR features that define specific modes of translation of functionally related MTOR-sensitive mRNAs

SUPPLEMENT

Includes:

Supplementary methods

Supplementary figures and legends

Supplementary references

Supplementary methods:

Conversion of bound ribosomes to sedimentation distance

The relationship between sedimentation distance and the number of bound ribosomes was obtained by manually identifying the sedimentation distances for 1 to 7 ribosomes using a polysome-tracing obtained as described previously (Gandin et al. 2014). The lm function in R (r-project.org) was then used to calculate the intercept and the slope for the regression of sedimentation distance to log2 number of bound ribosomes. This allowed for conversion between numbers of bound ribosomes and sedimentation distances.

Simulation of ribosome association

The range of ribosome association was simulated by sampling from a normal distribution with mean and [sd] (3[3], 4[4], 5[5], 6[6], 7[7], 8[8], 9[9] and 10[10] for the control condition and 1[1.5] under MTOR inhibition). The control condition parameters were based on the observation that ribosome binding under the control condition can be simulated using a normal distribution with a coefficient of variation equal to 1 (**Sup. Fig. 2**). For the

condition with MTOR inhibition a coefficient of variation of 1.5 was selected because this provided the best fit to non-TOP genes under MTOR suppression as quantified across the polysome gradient using qPCR (**Sup. Fig. 2**).

Similarly, for the TOP and non-TOP simulations (notice that non-movers are only used in the simulation presented in **Fig. 1J-K** and not **Fig. 1D-I** or **Sup. Fig. 4**), ribosome binding was simulated by sampling from a normal distribution with a mean and [sd] (3[3] for non-TOP, 5[5] for TOP and 5[5] for non-mover under the control condition; and 1[1.5] for non-TOP or TOP and 5[5] for non-mover under MTOR inhibition) using the rnorm function in R. TOP (under control condition) and non-TOP (under control and MTOR inhibition conditions) parameters were means obtained after fitting normal distributions to 3 TOP or 3 non-TOP genes quantified across the polysome gradient using qPCR (**Sup. Fig. 2**). Parameters for non-movers were obtained by fitting a normal distribution to the polysome-tracing (which is equivalent to a mean of all mRNAs) (**Sup. Fig. 2**). Because TOP mRNAs shift to the sub-polysome fractions to a large extent, which is poorly modelled using normal distributions, we used a mean ribosome-association of 1 and an standard deviation of 1.5 to represent the ribosome association under the condition where MTOR is inhibited (i.e. the same as for non-TOP although the shifts for TOP are more extreme). Values >0 were kept and converted to integers to resemble ribosome binding. Only integer values corresponding to a sedimentation distance <75 mm and >0mm were kept which equals the maximum and minimum sedimentation distance, respectively, in the sucrose gradient used (Larsson et al. 2012). For polysome-profiling a cut-off for isolation of heavy polysomes corresponding to >3 bound ribosomes as performed previously (Larsson et al. 2012) was estimated to 44 mm and the

proportion of sampled data points with a sedimentation distance >44 mm was calculated. For ribosome-profiling the sedimentation distances between 0 and 75 mm were re-converted to number of bound ribosomes and the mean number of bound ribosomes was calculated. 300 000 sampled data points were simulated to generate distributions as shown in **Fig. 1D** and **Sup. Fig. 3**.

Simulating a comparison of efficiency in identification of mRNAs showing different shifts as differentially translated by ribosome- and polysome-profiling

To compare polysome-profiling to ribosome-profiling regarding identification of mRNAs with different shifts (i.e. 3-10 ribosome vs 1 ribosome) or TOP and non-TOP mRNAs as differentially translated we sampled N genes (N=1000) with 3 replicates for each condition (control or MTOR inhibition) and RNA type (across all shifts or for TOP and non-TOP). Individual data points (i.e. per gene, condition and replicate) were calculated as described above but instead of using 300 000 data points to obtain a proportion of efficiently translated and mean number of bound ribosomes, 15 data points were generated that passed the filtering indicated above. This allowed for such calculations while maintaining variability across replicates. The resulting data (i.e. both proportions of efficiently translated mRNA and mean number of ribosomes) were log2 transformed and a t-statistic and fold change were calculated between control and MTOR inhibition conditions for all shifts or TOP or non-TOP. The resulting p-values or fold-changes were combined across all shifts or TOP and non-TOP followed by ranking. The proportions of genes from each shift or TOP or non-TOP was then calculated among the 30% genes with most negative log2 fold-changes (i.e. suppressed by MTOR inhibition) or lowest p-values. N was set to 1000 to obtain stable

proportions at the extreme ends of the ranked list. All simulations were performed 4 times and the data presented represents means and standard deviations from these 4 replicated simulations. In addition to these simulations we also modulated a range of parameters to assess the robustness. These simulations are explained and displayed in **Sup. Fig. 3**.

Simulating the impact of changes in TOP mRNA translation on observed fold-changes for TOP and non-TOP mRNAs

To simulate the effect of changes in translation of TOP mRNAs on TOP and non-TOP mRNAs we included several parameters in addition to the mean and the standard deviations as described above for TOP, non-TOP and non-movers under control or MTOR inhibition conditions. The first parameter was expression level and we calculated reads per kilo base per million mapped reads (rpkm) for the control condition and poly-A RNA-seq data obtained by Hsieh et al (Hsieh et al. 2012) but re-analyzed as described below. The rpkm measure attempts to correct data across genes for differences in length of the mRNA. Thus rpkm values approximate relative expression levels across genes. The mean rpkm values used were 34 for non-movers (i.e. detected but not regulated), 51 for non-TOP (the genes identified by Larsson were used to approximate this parameter as this data set was strongly enriched for non-TOP mRNAs) and 626 for TOP (the genes identified by Hsieh were used to approximate this parameter as this data set was strongly enriched for TOP mRNAs) mRNAs as estimated from the Hsieh et al. study (Hsieh et al. 2012) (**Fig. 1A**). The second parameter is the proportion of all expressed genes that are TOP, non-TOP or non-movers. The non-TOP proportion was set to the proportion of detected genes [rpkm>0.2 (Ramskold et al. 2009)] under both poly-A data replicates of the control condition in the study by Hsieh et al. (Hsieh

et al. 2012) that were identified as differentially translated by polysome-profiling (Larsson et al. 2012), i.e. 2.4%. During the simulation the proportion of TOP mRNAs varied from 0% to 5% with increments of 0.5% and non-movers were the remaining population. For each simulation condition (i.e. from 0% to 5% TOP) proportions of translationally active mRNAs and means of number of bound ribosomes were obtained as described above but with 30 000 sampled data points. This was repeated 100 times per simulation condition to obtain stable across iteration means of proportions of efficiently translated mRNAs and mean number of bound ribosomes. For both control and MTOR inhibition conditions, and RNA type (TOP, non-TOP and non-mover) the obtained proportions of efficiently translated mRNAs or mean number of mRNAs were multiplied by the proportion of all expressed genes belonging to that RNA type and the expression level for that RNA type. This corresponds to a situation when absolute expression levels could be obtained. To obtain relative levels such values were normalized by dividing by the sum across TOP, non-TOP and non-movers per condition separately (i.e. control or MTOR inhibition). Fold-changes between control and MTOR inhibition conditions were then calculated for absolute (i.e. before normalization) and relative (i.e. after normalization) data.

Simulating the impact of changes in global translation on observed fold-changes for TOP and non-TOP mRNAs

To simulate the effect of global reduction in translation we used the same settings as described for the TOP abundance simulation and in addition set the TOP proportion to the proportion of genes detected as differentially translated by (Hsieh et al. 2012) as compared to those detected (i.e. 0.9% **Fig. 1A**). Because non-TOP mRNAs were 2.4% the proportion of

non-movers was set to 96.7%. We then gradually introduced a global reduction in translation by reducing the mean number of bound ribosomes under the condition of MTOR inhibition for non-movers only. Absolute and relative fold-changes were obtained for each simulated condition as described above.

Preparation of nanoCAGE libraries

NanoCAGE libraries were prepared as described (Salimullah et al. 2011) previously but with a number of modifications as follows:

RNA extraction

Total RNA was extracted from MCF7 cells using TRI-reagent (Sigma-Aldrich, Stockholm, Sweden) and further purified with the RNeasy MinElute Cleanup kit (Qiagen, Sollentuna, Sweden) according to manufacturer's recommendations. RNA quantity was measured by target-specific fluorescence (Qubit; Life technologies, Stockholm, Sweden) and its quality was assessed with Agilent Bioanalyzer (Agilent Technologies, Kista, Sweden). RNA had an integrity number (RIN) > 9.

Template-switching reverse-transcription

1 µl 0.66 M D-Trehalose (Sigma-Aldrich), 3.3 M of D-Sorbitol (Sigma-Aldrich) with 10 µM MS-RanN6 oligonucleotide (Sigma-Aldrich); all oligos are listed below) and an equimolar mixture (100 µM) of two template-switching oligonucleotides (TS) with different barcodes (BC) (Integrated DNA Technologies, Leuven, Belgium) was mixed with 1 µl of total RNA (50 ng) and heat-denatured for 5 min at 65° C and then chilled on ice. Reverse transcription was carried out in a total volume of 10 µl with the following components: 1 x first-strand buffer (Life technologies, Stockholm, Sweden), 0.5 mM DTT (Life technologies, Stockholm,

Sweden), 625 µM dNTP mix [TaKaRa (th.geyer, Malmö, Sweden)], 1 M betaine (Sigma-Aldrich, Stockholm, Sweden) and 100 units of SuperScript III (Life technologies, Stockholm, Sweden) (25° C for 5 min, 42° C for 60 min, 72° C for 15 min and chilled on ice). Agencourt RNAClean XP magnetic beads (Beckman Coulter, Bromma, Sweden) were used to remove primer dimers according to the manufacturer's instructions but with a 1:1 (v:v) bead:sample ratio. The final elution volume was 40 µl (nuclease-free water).

Second-strand cDNA synthesis by semi-suppressive PCR amplification

To determine the optimal number of cycles needed for second-strand synthesis by semi-suppressive PCR a diagnostic qPCR was performed. 8.5 µl of 1 x SYBR Premix Ex Taq [TaKaRa (th.geyer, Malmö, Sweden)] with 100 nM of MS-dir 1F and 100 nM of MS-dir 1R oligonucleotides (Sigma-Aldrich, Stockholm, Sweden) was distributed in a 96 well plate (Bio-Rad, Sundbyberg, Sweden) and 1.5 µl of cDNA was added. Each cDNA sample was amplified in triplicate (95° C for 5 min, [65° C for 15s and 68° C for 2 min] x 40 cycles; CFX96 Touch, Bio-Rad, Sundbyberg, Sweden). The cycle threshold (CT) value was determined as the number of cycles required for the fluorescent signal to exceed the background level. For semi-suppressive PCR, 15 µl of purified first-strand cDNA was prepared in a final volume of 100 µl containing 1 x ExTaq Buffer [TaKaRa (th.geyer, Malmö, Sweden)], 200 µM dNTPs [TaKaRa (th.geyer, Malmö, Sweden)], 100 nM of MS-dir 1F and 100 nM of MS-dir 1R oligonucleotides (Sigma-Aldrich, Stockholm, Sweden), and 5 U of ExTaq in duplicates (a cycle number equal to the identified CT value plus 6 additional cycles was used for second strand synthesis). The final product (pooled duplicates) was purified in a 1:1 (v:v) mixture with the Agencourt AMPure XP beads (Beckman Coulter, Bromma, Sweden) according to manufacturer's instructions. The final elution volume was 30

µl (nuclease-free water). cDNA quantity was measured by target-specific fluorescence (Qubit; Life technologies, Stockholm, Sweden) and diluted to 10 ng/µl for subsequent steps. The absence of primer dimers was verified using a 1% agarose gel.

Addition of sequencing adapters and indexes to libraries

The addition of Illumina-specific adaptors needed for sequencing was done by PCR. 80 ng of purified cDNA was prepared in a 50 µl reaction containing 1 x KAPA HiFi buffer [KAPA Biosystems (Techtum, Umeå, Sweden)], 0.3 mM KAPA dNTP mix buffer [KAPA Biosystems (Techtum, Umeå, Sweden)], 400 nM of MS-dir 2F, 400 nM of MS-6b-dir 2R (Sigma-Aldrich, Stockholm, Sweden) and 0.2 U KAPA HiFi DNA polymerase buffer [KAPA Biosystems (Techtum, Umeå, Sweden)]. The following thermal cycling program was used: 95° C for 1 min, (95° C 15 s, 55° C 10 s, 68° C 2 min) x 1, (95° C 15 s, 65° C 10 s, 68° C 2 min) x 6. All samples were amplified in triplicates. The final product (pooled triplicates) was purified in a 0.6:1 (v:v) mixture with the Agencourt AMPure XP beads (Beckman Coulter, Bromma, Sweden) according to manufacturer's instructions. The final elution volume was 15 µl (2.5nM of Tris-HCL; pH 8.5). cDNA quantity was measured by target-specific fluorescence (Qubit, Life Technologies, Stockholm, Sweden). Final library size distribution analysis was performed using the High-sensitivity DNA kit on a Bioanalyzer (Agilent Technologies, Kista, Sweden).

Library sequencing

Prior to sequencing, all sample-concentrations were adjusted to 10 nM following Illumina's technical note for library validation and cluster density optimization. Adjusted samples were then pooled together accordingly, clustered using onboard clustering and sequenced on HiSeq2500 (Illumina, St Diego, California, US) with a 1x50 or 1x100 setup in Rapid Run

mode. After each cycle, image analysis and base calling was performed using CASAVA software suit.

Primers used for nanoCAGE sequencing

1st-strand_F; MS-FP_BC: 5'-TAGTCGAACTGAAGGTCTCCAGCA [barcode_sequence*]TATA(rG)(rG)(rG)-3'

1st-strand_R; MS-Ran6: 5'-TAGTCGAACTGAAGGTCTCCGAACCGCTCT TCCGATCTNNNNNN-3'

2nd-strand_F; MS-dir1F: 5'-TAGTCGAACTGAAGGTCTCCAGC-3'

2nd-strand_R; MS-dir1R: 5'-TGACGTCGTCTAGTCGAACTGAAGGTCTCCGAACC-3'

Adaptor_F; MS-dir2F: 5'-AATGATACGGCGACCACCGAGATCTACACTAGT CGAACTGAAGG-3'

Adaptor_R; MS-6b-dir2R: 5'-CAAGCAGAAGACGGCATACGAGAT (Index_reverse-complement**) GTGACTGGAGTTCAGACGTGTGCTCTTCCGATCT-3'

Sequence_F; MS-seqF: 5'-TAGTCGAACTGAAGGTCTCCAGCA-3'

*barcode_sequences: ATCGTC, GAGTGA, TCGCGT and CTGAGC.

** Index sequences: GCCTAA and TGGTCA.

Analysis of nanoCAGE data

nanoCAGE reads corresponding to transcription start sites (TSS) were extracted, de-multiplexed and reads aligning to ribosomal RNA were removed using TagDust 2.13 (Lassmann 2015). The resulting reads were aligned to hg19 using Bowtie 1.0.1 (Langmead et al. 2009) allowing 2 mismatches (default parameters). Uniquely aligned reads (using "m" and

"best" parameter in bowtie) and reads that failed to align to hg19 were then aligned to RefSeq 5' UTRs plus 78 bases of upstream genomic sequence and 78 bases of downstream sequence using bowtie as above but without the "m" parameter to allow reads to map to multiple isoforms. The alignments were then trimmed to remove sequence mismatches within the first two bases. Reads originating from strand invasion were removed as described (Tang et al. 2013) with the "-e" parameter set to 2 and sequences from the same set of 5' UTRs with 78 bases upstream genomic and 78 bases downstream sequence. All suggested TSS were collected and used in a sampling procedure where increasing number of reads were iteratively (n=5) sampled followed by determination of the number of RefSeqs (>50 reads) or peaks (>5 reads) that were detected (**Fig. 2B**). All high confident RefSeqs (>50 reads) and peaks (>5 reads at the exact same position) where then collected and 5' UTR lengths were calculated either by determining the length suggested by the position that obtained the largest number of reads (mean if 2 or more positions had the same number of reads) or by determining the mean length suggested by all reads. To identify TOP elements only the position with the largest number of reads was considered. Sequence at the peak position ±2 bases was searched for TOP elements (CYYYY where Y is C or T). The proportion of genes with at least one RefSeq 5' UTR containing a TOP element in PP242 sensitive mRNAs identified by polysome-profiling (Larsson et al. 2012) could then be determined. GAGE (Luo et al. 2009) was used to assess whether genes targeting specific cellular functions were enriched at the top or bottom of a list ranked by nanoCAGE peak or mean 5' UTR length or those 5' UTR lengths suggested by the RefSeq database. Biological processes as defined by GEO were used as inputs and functions that showed a FDR<0.1 were considered significant. TISU elements were searched for in all human mRNAs as defined by UCSC using the

degenerate IUPAC sequence SAASATGGCGGC (Elfakess and Dikstein 2008; Elfakess et al. 2011), where ATG is the start codon, and allowing for 2 mismatches. Genes for which any of the mRNA isoforms contained a TISU were annotated as containing a TISU.

Reanalysis of ribosome-profiling data on MTOR sensitive translation

To take advantage of recent improvements in aligning RNA-seq reads to the genome we realigned and recalculated expression data for ribosome-profiling studies. Raw data were downloaded from GEO (GSE35469 and GSE36892) (Hsieh et al. 2012; Thoreen et al. 2012). Hisat 0.1.5 (Kim et al. 2015) was used to align the first 25 bases of each read to the hg19 (GSE35469) or mm9 (GSE36892) genomes using default settings. Counts and rpkms were calculated as described using default settings for coding genes as defined by RefSeq (Ramskold et al. 2009). Differential expression was analyzed for data from ribosome protected fragments between control and MTOR inhibition conditions and a range of filters for the minimum number of reads for each of the control condition replicates. Both edgeR (Robinson et al. 2010) (using the exact test on raw counts) and a random variance model (Wright and Simon 2003) t-test (2-sided t-test on log2 transformed centered counts) were used for analysis of differential expression. Babel (Olshen et al. 2013) was used to identify changes in ribosome protected fragments that were independent of changes in poly-A RNA using default settings. RVM and edgeR p-values were adjusted using the Benjamini Hochberg False Discovery Rate (FDR) method (Benjamini and Hochberg 1995) while FDRs for babel were default FDRs reported.

Western blotting and antibodies.

Cells were scraped in ice-cold PBS (pH 7.4), washed by centrifugation (800 x g/5 minutes at 4^{o}C) and lysed on ice in RIPA buffer [20 mM Tris-HCl (pH 7.5), 150 mM NaCl, 1 mM Na_2EDTA, 1 mM EGTA, 1% (v/v) NP-40, 1% (w/v) Na-deoxycholate, 0.1% (w/v) SDS, 2.5 mM Na-pyrophosphate, 50 mM NaF, 20 mM β-glycerophosphate, 1mM Na_3VO_4] supplemented with 1X complete protease inhibitors (Roche) for 30 minutes with occasional vortexing. After lysis, cellular debris was removed by centrifugation at (16,100 x g/20 minutes at 4^{o}C) Protein concentrations in cell extracts were determined using Pierce BCA Protein Assay Kit (Thermo Fisher Scientific). Protein extracts (20-80 μg of protein) were resuspended in Laemmli buffer, separated by sodium dodecyl sulfate-polyacrylamide gel electrophoresis (7.5 and 15% polyacrylamide) and transferred to nitro-cellulose membrane (Bio-Rad) using a wet-transfer apparatus from Cleaver according to the manufacturer's instructions. To detect proteins of interest we used the following primary antibodies and dilutions: anti-ACTB (Clone AC-15) #A1978 (1:5000) from Sigma (Saint Louis, Missouri, USA); anti-EIF4EBP1 (53H11) #9644 (1:2000), anti-p-EIF4EBP1 (S65) (174A9) #9456 (1:1000), anti-p-RPS6 (S240/244) #2215, anti- CCND3 (DCS22) #2936 (1:1000), anti-EIF4G1 #2858 (1:1000), anti-MAP1LC3A #4599 (1:1000), and anti-MAP1LC3B #3868 (1:1000) all from Cell Signaling Technologies (Danvers, MA, USA), anti-RPS6 (C-8) #sc-74459 (1:2000), anti-MCL1(H-260) #sc-20679 (1:200), anti-BCL2 #Sc-783 (1:500) from Santa Cruz Biotechnologies (Dallas, Texas, USA), anti-NDUFS6[EPR15957] #ab195807 (1:1000), anti-ATP5G1 #ab96655 (1:1000), anti-ATP50 [4C11C10D12] #ab110276 (1:500), (1:1000), anti-EIF4A1 #ab31217 (1:1000), and anti-EIF4A2 #ab31218 (1:1000), all from Abcam (Cambridge, MA, USA), anti-EIF4E #610269 (1:1,100) from BD Biosciences (San

Jose, CA, USA), anti-BIRC5 #SURV11-S (1:500) from Alpha Diagnostics (San Antonio, Texas, USA), and anti-UQQC2/MNF1 #LS-C170376 (1:1000) from LS Bio (Seattle, WA, USA). All primary antibodies were incubated in 5% (w/v) BSA in 1 x TBS/0.5%Tween20 (Sigma) over night at 4^{o}C. Secondary anti-mouse-HRP and anti-rabbit-HRP antibodies (Amersham) were used at 1:10,000 dilution in 5% (w/v) non-fat dry milk in 1 x TBS/0.5%Tween 20 for 1 hour at room temperature. Signals were revealed by chemiluminescence (ECL, GE Healthcare) on HyBlot ES X-ray film from Denville Scientific (Holliston, MA, United States). Where possible, membranes were stripped and re-probed. In the cases where this was not possible (e.g. wherein the phospho- and total-antibodies or antibodies recognizing same proteins were used and significant signal remained on the membrane after striping), same lysates were ran simultaneously on duplicate gels, and probed with phospho- and total-antibodies.

Primers used for RT-qPCR analysis.

Following primers were designed using NCBI Primer-BLAST (http://www.ncbi.nlm.nih.gov/tools/primer-blast/) such that the Tm difference was less than 3^{o} C and whenever possible primer pairs were separated by at least one intron. Primers were obtained from Integrated DNA Technologies (IDT, Coralville, Iowa, USA) and their sequences and size of the amplicons are listed below:

CCDN3 human forward: 5'- CTGGATCGCTACCTGTCTTG-3'

CCDN3 human reverse: 5'-TCCCACTTGAGCTTCCCTAG -3'

Amplicon: 200 nt

MCL1 human forward: 5'-CGTAACAAACTGGGGCAGGA-3'

MCL1 human reverse: 5’-CAAACCCATCCCAGCCTCTT-3’

Amplicon: 176 nt

BCL2 human forward: 5’-TGAGTTCGGTGGGGTCATGT-3’

BCL2 human reverse: 5’-CGTACAGTTCCACAAAGGCATC-3’

Amplicon: 155 nt

BIRC5 human forward: 5’-TTCAAGGAGCTGGAAGGCTG-3’

BIRC5 human reverse: 5’-CGCACTTTCTCCGCAGTTTC-3’

Amplicon: 251 nt

ATP5O human forward: 5’-CTCTCTTCCCACTCGGGTTT-3’

ATP5O human reverse: 5’-TGACCACAGAGGTACTGAAGCA-3’

Amplicon: 107 nt

NDUFS6 human forward: 5’-TCGGTT TGTAGGTCGTCAGA-3’

NDUFS6 human reverse: 5’-GCATGTGCCGGTTTTTGTTTC-3’

Amplicon: 96 nt

ATP5G1 human forward: 5’-GACCGCCGGGGCATTATTCA-3’

ATP5G1 human reverse: 5’- CCTGGAGTGGGAAGTTGCTGT-3’

Amplicon: 140 nt

UQCC2 human forward: 5’-AAACACAAGTACCCTCGCCC-3’

UQCC2 human reverse: 5’-ATCCTCCTCAGGACCCTTGG-3’

Amplicon: 165 nt

ACTB human forward: 5’-ACCACACCTTCTACAATGAGC -3’

ACTB human reverse: 5’- GATAGCACAGCCTGGATAGC-3’

Amplicon: 163 nt

GAPDH human forward: 5'-AATCCCATCACCATCTTCCA-3'

GAPDH human reverse: 5'-TGAGTCCTTCCACGATACCA-3'

Amplicon: 310 nt

ODC1 human forward: 5′- GAAGAGATCACCGGCGTAAT-3′

ODC1 human reverse: 5′- TTAACTGCAAGCGTGAAAGC-3′

Amplicon: 122 nt

RPL32 (#PPH02371C), *RPS6* (#PPH00790E) and *EEF2* (#PPH09956A) primers were obtained from Qiagen (Toronto, Ontario, Canada)

siRNAs and shRNAs

Small interfering RNA (siRNA) targeting *EIF4A1* (HSC.RNAI.N001416.12.3), *EIF4A2* (HSC.RNAI.N001967.12.3), *EIF4E* (DUPLEX: 5'-rArGrArGrUrGrGrArCrUrGrC rArUrUrUrArArArUrUrUGAT-3'; 5'-rArUrCrArArArUrUrUrArArArUrGrC rArGrUrCrCrArCrUrCrUrGrC-3') or scrambled negative control were obtained from Integrated DNA technology (IDT, Coralville, Iowa, USA). siRNA were transfected using Lipofectamine 2000 (Invitrogen, Burlington, Ontario, Canada) at the final concentration of 10 nM according to the manufacturer's instructions and as previously described (Topisirovic et al. 2009). pLKO.1-Puro vectors encoding *EIF4A1* and *EIF4A2* shRNAs were obtained from Sigma, Oakville, Ontario, Canada (Mission-TRCN0000288728 (sh-EIF4A1 (A)); and TRCN0000288729 (sh-EIF4A1 (B)). Lentiviral shRNA infections were carried out as previously (Dowling et al. 2010).

Generation of luciferase reporters and luciferase assays.

ATP5O(5'UTR)-FF, UQCC2(5'UTR)-FF and NDUFS6(5'UTR)-FF constructs were generated by inserting ATP5O 5'UTR (5'-GGGAGAAG-3'), UQCC2 5'UTR (5'-GGGGCCCAAG-3') and NDUFS6 5' UTR (5'-GGGTCAAAGGCCAGCGGCGCAAA-3') into pCDNA3-Firefly Luciferase plasmid (Kim and Chen 2000) via QuickChange site-directed mutagenesis (Stratagene, Santa Clara, California, USA) according to the manufacturer's instructions. Following primers were used:

ATP5O 5UTR_F: 5'-TACCGAGCTCGGATCCAAGGGAGAAGATGGAAGACGC CAA-3'

ATP5O 5UTR_R: 5'-TTGGCGTCTTCCATCTTCTCCCTTGGATCCGAGCTCG GTA-3'

UQCC2 5UTR_F: 5'-TACCGAGCTCGGATCCAAGGGGCCCAAGATGGAAGAC GCCAA-3'

UQCC2 5UTR_R: 5'-TTGGCGTCTTCCATCTTGGGCCCCTTGGATCCGAGCTCG GTA-3'

NDUFS6 5UTR_F: 5'TACCGAGCTCGGATCCAAGGGTCAAAGGCCAGCGGCGC AAAATGGAAGACGCCAA-3'

NDUFS6 5UTR_R: 5'-TTGGCGTCTTCCATTTTGCGCCGCTGGCCTTTGACCCTTG GATCCGAGCTCGGTA-3'

ATP5O(TISU)-FF construct was generated using the same strategy using following primers:

AUG TISU_F: 5'CGGATCCAAGGGAGAAGATGGCTGCCGCCAAAAACATA AAGAAAGG-3'

AUG TISU_R: 5'-CCTTTCTTTATGTTTTTGGCGGCAGCCATCTTCTCCCTTGGAT CCG-3'

Therefore, ATP5O(TISU)-FF construct is identical to ATP5O(5'UTR)-FF except in ATP5O(TISU)-FF 2nd and 3rd codon of Firefly Luciferase (i.e. codons immediately following

AUGi) were modified from GAAGAC to GCTGCC to generate the portion of TISU element of ATP5O downstream of AUGi (GCTGC). The following C was left to keep TISU in frame with the Firefly Luciferase ORF.

IRF7(5'UTR)-FF was generated by inserting murine IRF7 5' UTR (Colina et al. 2008) into pCDNA3-Firefly Luciferase plasmid using BamHI. The 3' BamHI site was then removed using QuickChange site-directed mutagenesis (Stratagene) to fuse the 5' UTRs with the AUG of the firefly ORF.

For ATP5O(5'UTR)-SL-FF constructs, 5'-AGCTAAGCTTGGGAGAAGGTCCACC ACGGCCGATATCACGGCCGTGGTGGACGGATCCGACT-3' and 5'-GACTGGATCCGTCCACCACGGCCGTGATATCGGCCGTGGTGGACCTTCT CCCAAGCTTAGCT-3' oligos (IDT, Coralville, Iowa, USA) containing ATP5O 5'UTR followed by the stem loop (this stem loop was described and characterized in (Babendure et al. 2006)) were annealed by heating for 2 min at 95^{o} C followed by cooling to room temperature. Annealed duplex was cloned into pCDNA-Firefly (Addgene) using BamHI and HindIII. Integrity of all constructs was verified by sequencing.

HEK293E cells were seeded in a 10 cm-Petri dish and transfected using 30 μL of Lipofectamine 2000 (Invitrogen), 600 ng of control Renilla (obtained from Y.Svitkin and N. Sonenberg) and 1.2 μg of the firefly luciferase constructs. The next day, cells were seeded in triplicate in a 24-well plate and translation of the indicated reporters was monitored 48 h post-transfection using Dual Luciferase Assay System (Promega, Madison, Wisconsin, USA) according to the manufacturer's instructions. For the siRNA experiments, cells were transfected with siRNAs 24 h prior to luciferase transfections, whereas the treatments with

250 nM torin1, 1 μM hippuristanol (hipp) or a vehicle (DMSO) were performed 48 h post-luciferase transfection and the luciferase activity was measured after 30, 90 and 180 min.

Cap (m^7GDP) pull-down assay

Cap-binding affinity assay was performed as previously described (Dowling et al. 2010). MCF7 cells were lysed in 2 volumes of Buffer B [50 mM MOPS/KOH (7.4), 100 mM NaCl, 50 mM NaF 2 mM EDTA, 2 mM EGTA, 1% NP40, 1% Na-DOC, 7 mM β-ME, protease inhibitors and phosphatase inhibitor cocktail 1 (both from Sigma-Aldrich)] on ice for 15 min with occasional vortexing. Lysate was cleared by centrifugation (16,100 x g/10 min at 4°C). m^7GDP was conjugated to the adipic acid dihydrazide agarose beads (Sigma-Aldrich) as described in (Edery et al. 1988). m^7GDP-agarose beads were equilibrated in Buffer C [50 mM MOPS/KOH (7.4), 100 mM NaCl, 50 mM NaF, 0.5 mM EDTA, 0.5 mM EGTA, 7 mM BME, 2 mM benzamidine or 0.5 mM PMSF, 1 mM Na_3VO_4 and 0.1 mM GTP]. Lysates were diluted (~500 μg of TCP) to 1 ml with Buffer C (in 2ml tube) and incubated with equilibrated m^7GDP-Agarose beads (~50μl of 50% slurry) for 20 min at 4°C on rotating wheel (end-over-end rotation). 20% of the lysate was used as the input. The beads were collected by centrifugation (500 x g/5 min at 4°C) and washed 4 times with 1.5 ml of Buffer C. Bound protein eluted with 0.2 mM m^7GDP, resuspended in SDS-PAGE loading buffer, ¼ of which was analyzed by Western Blotting along with the inputs (10%).

Cell counting

To assess equipotent doses of silvestrol and torin1, cells were seeded in culture plates and incubated for 24 h to allow attachment. Subsequently, seeding media was replaced with

treatment media and cells were grown for 24 or 72 h, at the end of which they were detached by trypsinization and collected. Cells were stained with trypan blue and counted using an automated cell counter (Invitrogen), which assessed the number of total and viable cells. Inhibition of cell proliferation was calculated as a percentage of DMSO-treated controls for each drug treatment. Experiments were carried out 3 times independently (n=3), with 4 technical replicates in each experiment.

Respiration assay

HEK293E cells were grown for 16 h in the presence of DMSO, silvestrol (25 nM) or torin1 (250 nM). For siRNA experiments, cells were transfected with control, EIF4E and EIF4A1 siRNA and analyzed 72 h later. Cells were trypsinized and counted using a TC10 automated cell counter. 7.5×10^5 or 1×10^6 were used for respiration measurements using a Digital Model 10 Clark Electrode (Rank Brothers, Cambridge, UK). Cells were incubated in 500 µL assay buffer media consisting of 50% HEK293E growth media and 50% PBS (pH 7.4) supplemented with 1 mM sodium pyruvate, 25 mM D-glucose, 20 mg/mL bovine serum albumin fraction V, 4 mM glutamine. Non-mitochondrial respiration represents respiration that is insensitive to myxothiazol (5 µM). Cells displayed no detectable non-mitochondrial respiration.

Flow cytometry analysis of mitochondria membrane depolarization

HEK293E cells were plated in 6-well plates and grown for 24 h, after which they were treated with torin1, silvestrol or DMSO control for 72 h. For siRNA experiments, cells were transfected with control, EIF4E and EIF4A1 siRNA, as indicated in the "Cell culture,

inhibitors, antibodies and siRNA" section. 72 h later, cells were grown in the absence of FBS and glucose for an additional 18 h to induce apoptosis. Cells were incubated with TMRE (tetramethylrhodamine, ethyl ester; 25 nM) for 20 min at 37° C in the presence of 5% CO2, trypsinized, washed twice with PBS and resuspended in PBS containing 0.2% FBS. As a positive control, cells in three wells were incubated for 10 min with mitochondrial membrane depolarizing agent FCCP (20 μM) prior to TMRE staining according to the manufacturer's instruction (Invitrogen). To exclude dead cells, cells were stained with DAPI 5 min prior to flow cytometry analysis. Samples were analyzed with a BD LSR Fortessa (BD Biosciences, San Jose, California, USA) at the LDI Flow Cytometry Core Facility. Fluorescence was detected by excitation at 561 nm and acquisition on the 582/15-A channel for TMRE and by excitation 405 nm and acquisition on the 450/50-A channel for DAPI. Data were analyzed using the FlowJo software. FCCP treated cells were considered as cells with depolarized mitochondrial membrane as per manufacturer's instruction (Invitrogen) and used to mark the position of the gate separating TMRE positive cells with integral mitochondria (MMP+) and TMRE negative cells harboring depolarized mitochondria (MMP-; **Fig. 7A; left panel**). Results were expressed as percentage of cells with depolarized mitochondrial membrane out of the total viable single cell population isolated using the SSC-A, FSC-A and FSC-H channels and excluding DAPI positive cells (**Fig. 7A; middle panel)** or as a cumulative TMRE signal (**Fig.7A; right panel**). Experiments were carried out 3 times independently (n=3), with 2 technical replicates in each experiment.

Flow cytometry analysis of mitochondrial mass (MitoTracker Green Assay)

HEK293E cells were plated in 6-well plates and grown for 24 h, after which they were treated with torin1, silvestrol or DMSO control for 16 h. For siRNA experiments, cells were transfected with control, EIF4E and EIF4A1 siRNA and analyzed 72 h later. Cells were trypsinized, counted and 100,000 cells were stained using MitoTracker Green (400 nM) for 20 min in the dark as per the manufacturer's instructions (MitoTracker Green FM, ThermoFisher Scientific). Samples were analyzed with a BD LSR Fortessa (BD Biosciences, San Jose, California, USA) at the LDI Flow Cytometry Core Facility. Fluorescence was detected by excitation at 488 nm and acquisition on the 530/30-A channel. Experiments were carried out 3 times independently (n=3), with 3 technical replicates in each experiment.

Flow cytometry analysis of apoptotic cells

HEK293E cells were plated in 6-well plates and grown for 24 h, after which they were treated with torin1, silvestrol or DMSO control for 72 h. For siRNA experiments, cells were transfected with control, EIF4E and EIF4A1 siRNA. 72 h later, cells were grown in the absence of FBS and glucose for an additional 18h to induce apoptosis. Cells were trypsinized, counted and 100,000 cells were stained using Annexin V-FITC and PI for 20min in the dark as per the manufacturer's instructions (FITC Annexin V Apoptosis Detection Kit, BD Biosciences). Samples were analyzed with a BD LSR Fortessa (BD Biosciences, San Jose, California, USA) at the LDI Flow Cytometry Core Facility. Fluorescence was detected by excitation at 488 nm and acquisition on the 530/30-A channel for FITC-Annexin V and by excitation at 561 nm and acquisition on the 610/20-A channel for PI. Cell populations were separated as follows: viable cells – Annexin V-/PI-; early apoptosis - Annexin V+/PI-; late

apoptosis Annexin V+/PI+low; necrotic/dead Annexin V+/PI+high and expressed as % of total single cells. Experiments were carried out 3 times independently (n=3), with 2 technical replicates in each experiment.

Supplementary Figures:

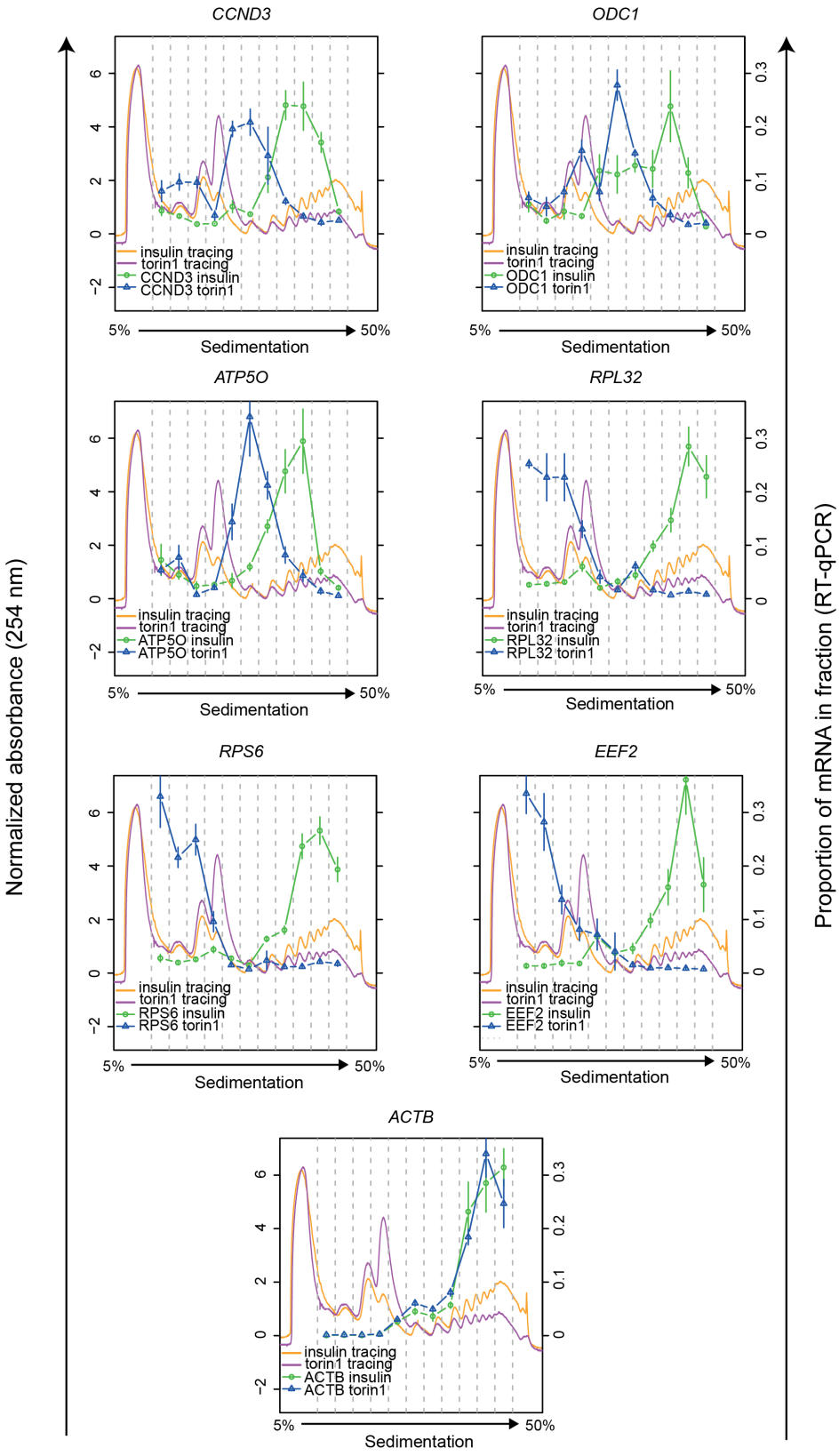

Sup. Fig. 1. Polysome shifts of non-TOP (*CCND3*, *ODC1* and *ATP5O*), TOP (*RPL32*, *RPS6* or *EEF2*), or control (*ACTB*) mRNAs in response to stimulation and inhibition of MTOR signaling by insulin and torin1, respectively. MCF7 cells were serum starved for 16 h and then stimulated with insulin (4.2 nM) or insulin in the presence of torin1 (250 nM) for 4 h, upon which cytosolic lysates were collected and fractionated on 5-50% sucrose gradients by ultracentrifugation. Absorbance at 254 nm was normalized to the area under 60S, 80S and polysomes and normalized absorbance profiles for insulin- (insulin tracings; orange) and torin1- (torin1 tracings; purple) treated cells are presented. RNA was isolated from each gradient fraction (grey broken lines), and subjected to RT-qPCR analysis. RT-qPCR data obtained from insulin (green) or torin1 (blue) treated cells are presented as a proportion of indicated mRNAs in each fraction (sum of all polysomal fractions for each mRNA was set to 1). Data are presented as means +/- SDs from 2 independent experiments each performed in triplicate.

A

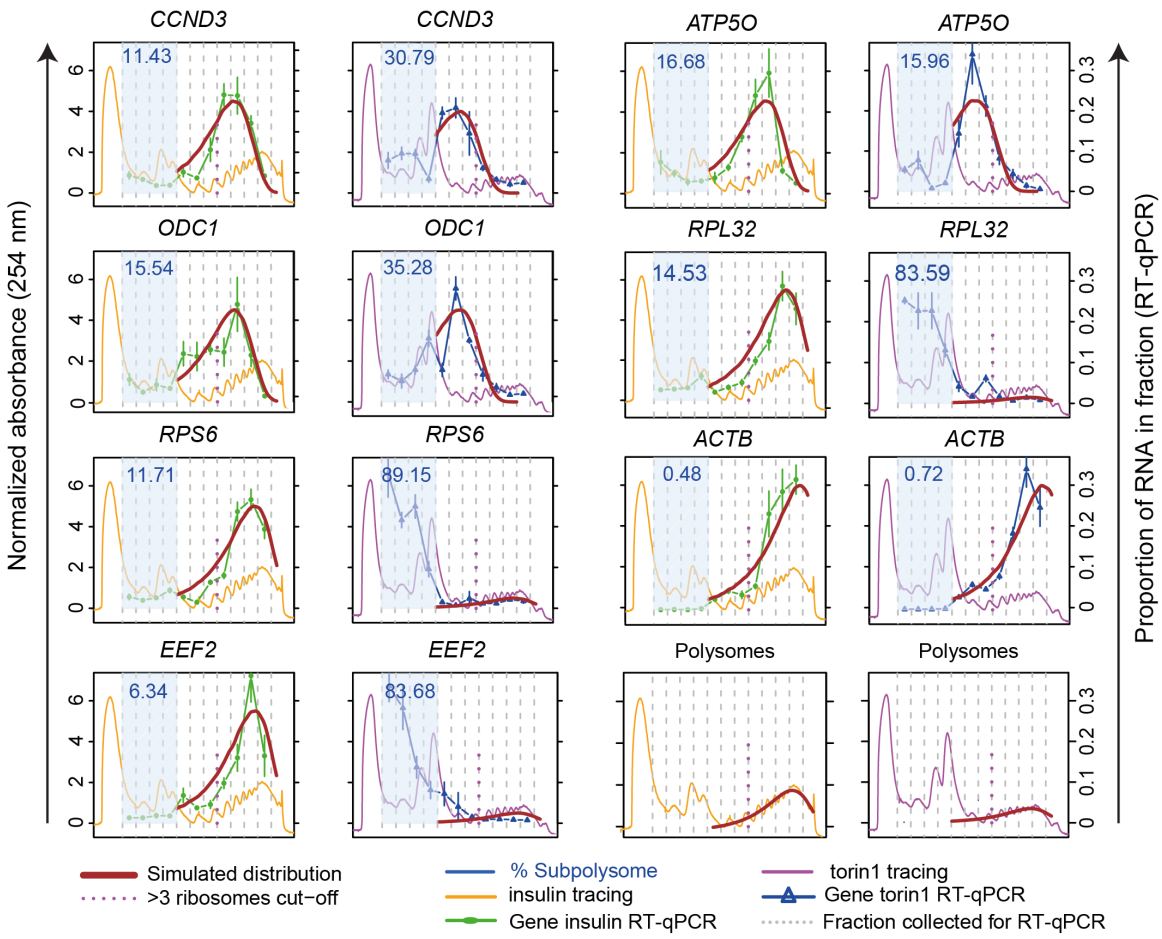

B

Gene	Condition	Mean of normal distribution	Standard deviation for normal distribution	Gene classification
RPS6	insulin	5	5	TOP
RPS6	torin1	5	5	TOP
RPL32	insulin	5	5	TOP
RPL32	torin1	5	5	TOP
EEF2	insulin	5	5	TOP
EEF2	torin1	5	5	TOP
ODC1	insulin	3	3	nonTOP
ODC1	torin1	1	1.5	nonTOP
CCND3	insulin	3	3	nonTOP
CCND3	torin1	1	1.5	nonTOP
ATP5O	insulin	3	3	nonTOP
ATP5O	torin1	1	1.5	nonTOP
ACTB	insulin	7	7	Control
ACTB	torin1	7	7	Control

C

Gene	Condition	Mean number of ribosomes	Mean standard deviation	Sub - polysome proportion (mean)	Sub- polysome proportion (sd)
TOP	insulin	5	5	10.9	4.2
nonTOP	insulin	3	3	14.5	2.8
polysomes	insulin	5	5	NA	NA
TOP	torin1	5	5	85.5	3.2
nonTOP	torin1	1	1.5	27.3	10.1
polysomes	torin1	5	5	NA	NA

Sup. Fig. 2. Parameters for simulation of shifts for TOP, non-TOP or non-mover mRNAs. (A) Polysome absorbance profiles (254 nm) from MCF7 cells serum starved for 16 h and then stimulated with insulin (orange) or insulin in the presence of torin1 (purple) for 4 h are shown (i.e. same as **Sup. Fig. 1**). Also shown are proportions of indicated mRNAs in each fraction of insulin- or torin1-treated cells as determined by RT-qPCR (blue or green lines; see **Sup. Fig. 1**). The percentage of each mRNA (according to the RT-qPCR data) that is found in the sub-polysome fractions (indicated by a light blue square) is indicated in blue. For each mRNA and condition we then fitted normal distributions (brown lines) to the RT-qPCR data within the polysome region. This was also done for the polysome-tracing (last two sub-panels). **(B)** A table of the parameters for the normal distributions for mRNAs shown in (**A**). **(C)** Means [i.e. from (**B**)] of numbers of ribosomes for indicated classes of mRNAs as well as their portion in sub-polysomal fractions in insulin- or torin1-treated cells. Also indicated are the parameters used to fit the normal distribution to the polysome tracings (which were used in simulations of non-movers as polysomes approximate the mean of all mRNAs).

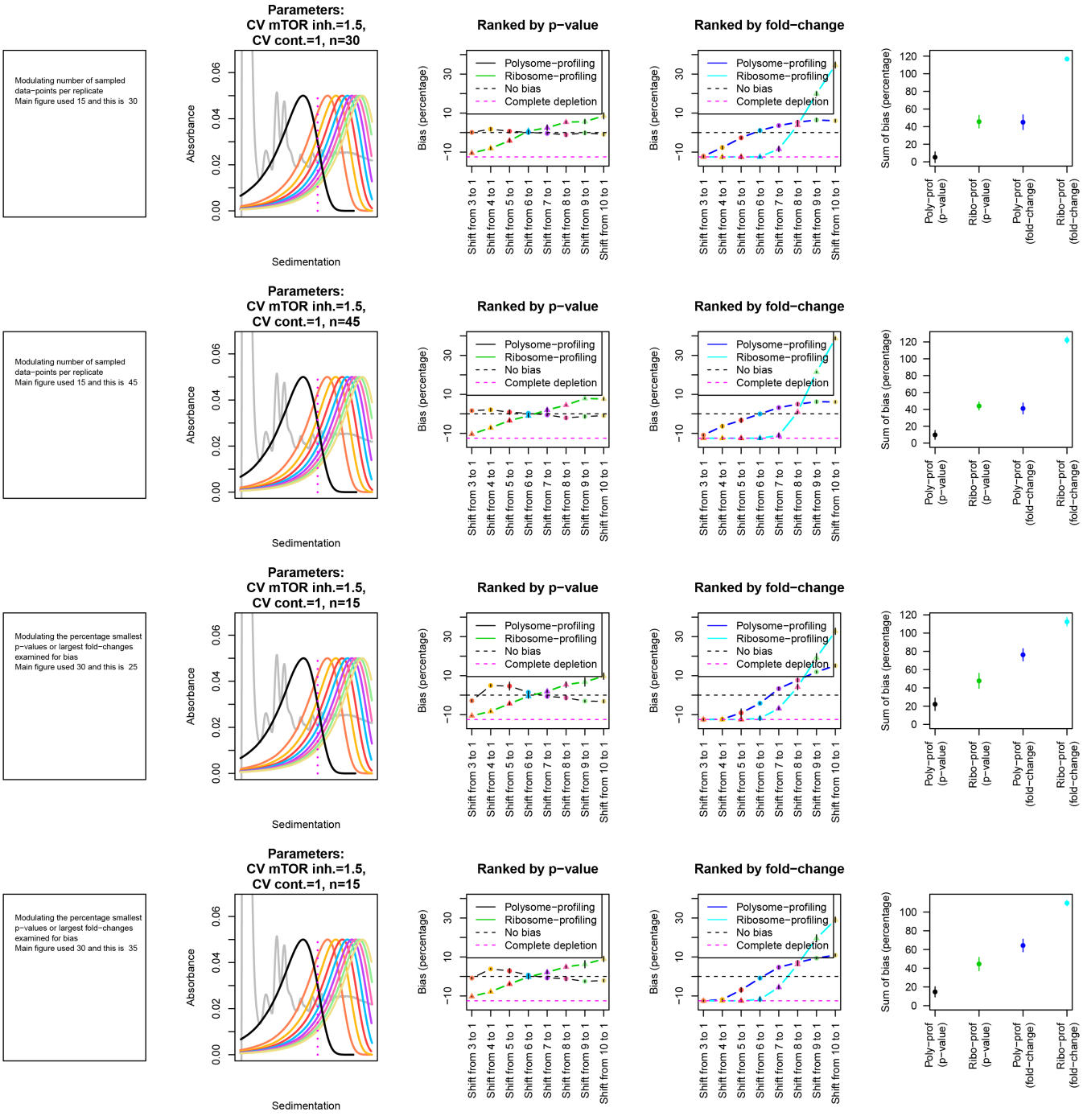
Modulating number of sampled data−points per replicate
Main figure used 15 and this is 30
Parameters:
CV mTOR inh.=1.5,
CV cont.=1, n=30
Absorbance
Sedimentation
Ranked by p−value
Ranked by fold−change
Bias (percentage)
Polysome−profiling
Ribosome−profiling
No bias
Complete depletion
Shift from 3 to 1
Shift from 4 to 1
Shift from 5 to 1
Shift from 6 to 1
Shift from 7 to 1
Shift from 8 to 1
Shift from 9 to 1
Shift from 10 to 1
Sum of bias (percentage)
Poly−prof (p−value)
Ribo−prof (p−value)
Poly−prof (fold−change)
Ribo−prof (fold−change)
Modulating number of sampled data−points per replicate
Main figure used 15 and this is 45
Parameters:
CV mTOR inh.=1.5,
CV cont.=1, n=45
Modulating the percentage smallest p−values or largest fold−changes examined for bias
Main figure used 30 and this is 25
Parameters:
CV mTOR inh.=1.5,
CV cont.=1, n=15
Modulating the percentage smallest p−values or largest fold−changes examined for bias
Main figure used 30 and this is 35
Parameters:
CV mTOR inh.=1.5,
CV cont.=1, n=15

Modulating the range of shifts that are included
Main figure used 3 to 10
and this is 3 to 6

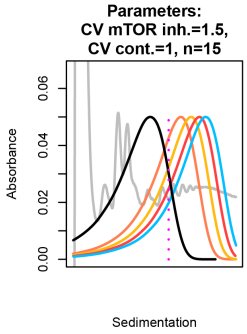

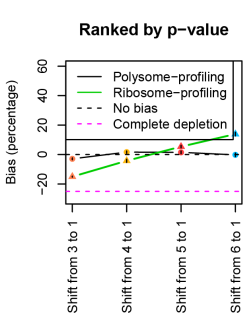

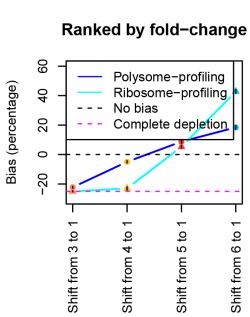

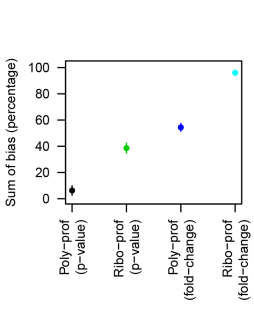

Modulating the range of shifts that are included
Main figure used 3 to 10
and this is 3 to 8

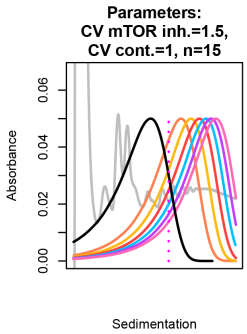

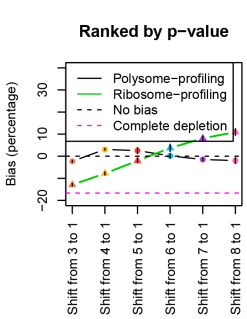

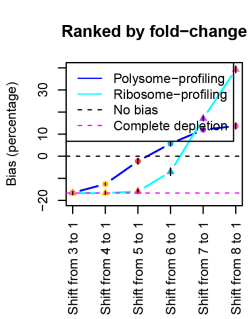

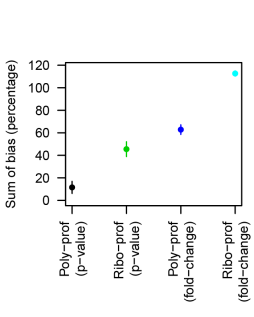

Modulating the mean under mTOR inhibition
Main figure used 1 and this is 1.5

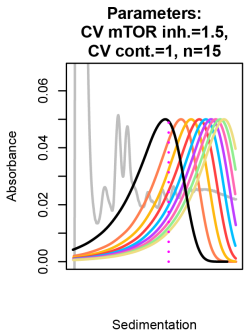

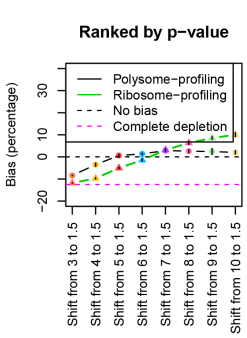

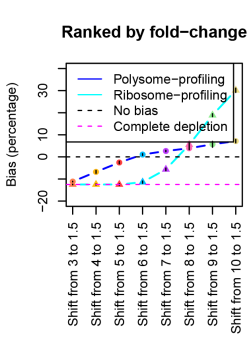

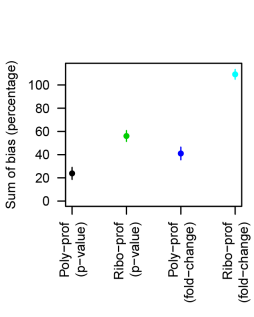

Modulating the mean under mTOR inhibition
Main figure used 1 and this is 2

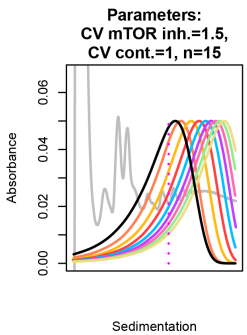

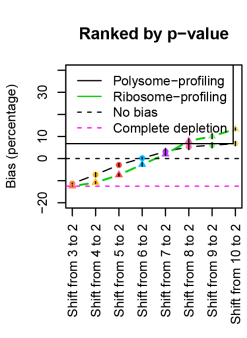

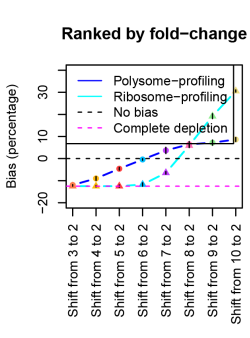

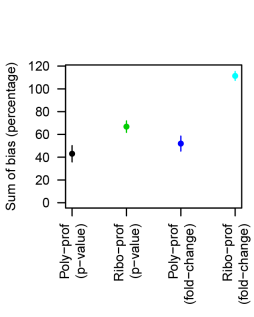

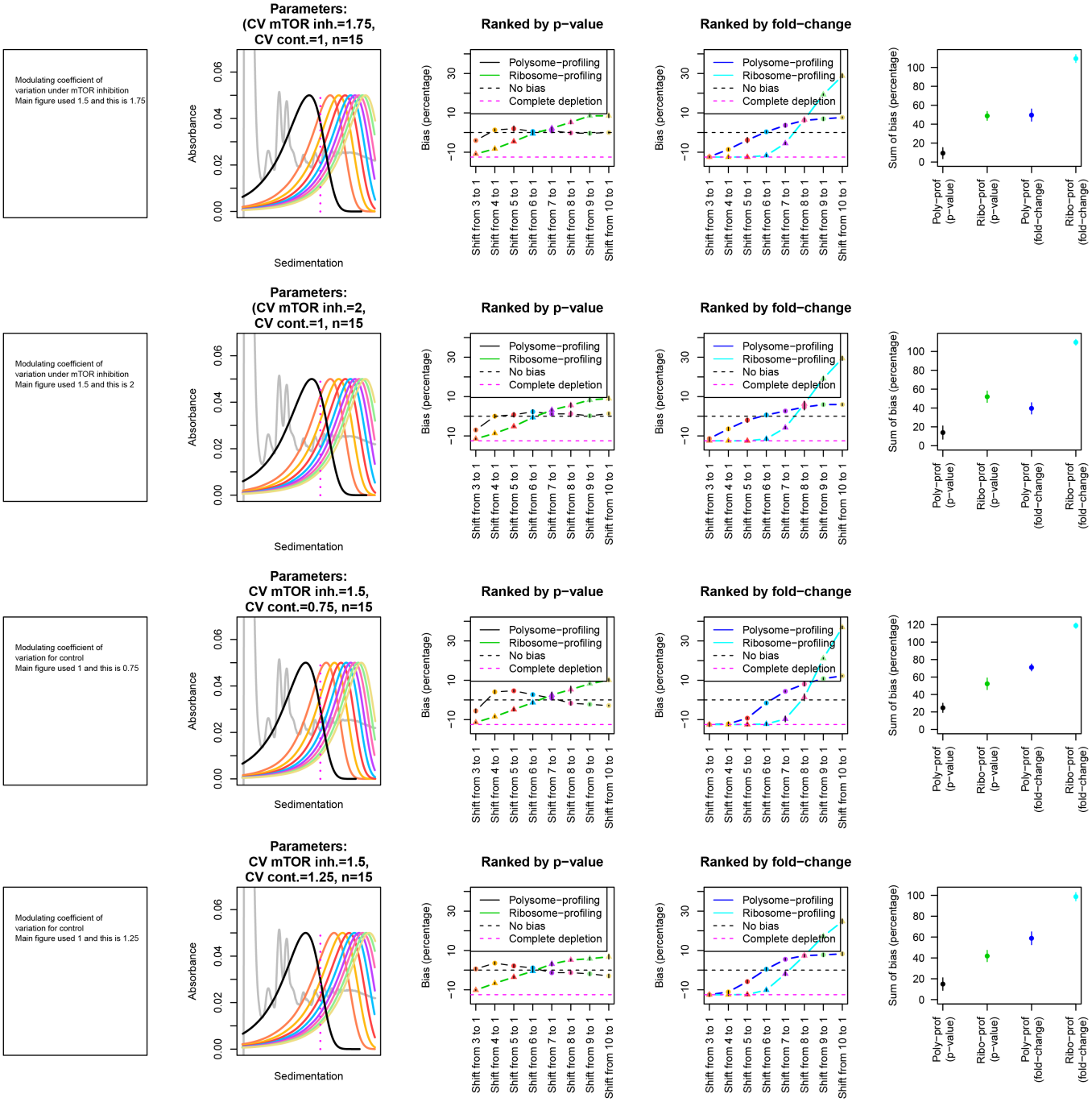
Modulating coefficient of variation under mTOR inhibition Main figure used 1.5 and this is 1.75
Parameters: (CV mTOR inh.=1.75, CV cont.=1, n=15
Absorbance
Sedimentation
Ranked by p−value
Ranked by fold−change
Bias (percentage)
Polysome−profiling
Ribosome−profiling
No bias
Complete depletion
Shift from 3 to 1
Shift from 4 to 1
Shift from 5 to 1
Shift from 6 to 1
Shift from 7 to 1
Shift from 8 to 1
Shift from 9 to 1
Shift from 10 to 1
Sum of bias (percentage)
Poly−prof (p−value)
Ribo−prof (p−value)
Poly−prof (fold−change)
Ribo−prof (fold−change)
Modulating coefficient of variation under mTOR inhibition Main figure used 1.5 and this is 2
Parameters: (CV mTOR inh.=2, CV cont.=1, n=15
Modulating coefficient of variation for control Main figure used 1 and this is 0.75
Parameters: CV mTOR inh.=1.5, CV cont.=0.75, n=15
Modulating coefficient of variation for control Main figure used 1 and this is 1.25
Parameters: CV mTOR inh.=1.5, CV cont.=1.25, n=15

Sup. Fig. 3. Simulations across a variety of alternative parameters.

Each row shows a simulation where one of the parameters used in the simulation in **Fig. 1D-I** is modulated. The first graph of each row indicates which parameter was modulated and how it was modulated; the second graph shows the resulting distributions; the third and fourth graphs show observed bias (i.e. obtained percentage of genes from each shift compared to expected percentage) across all shifts for an analysis ranked by p-value or fold-change, respectively; and the last graph shows the sums of bias across all shifts for each technology and analysis approach. The only parameter that affected the performance of polysome-profiling under p-value analysis was setting the ribosome association means under MTOR inhibition to 1.5 or 2 instead of 1 ribosome. Yet, in agreement with **Fig. 1G**, polysome-profiling still showed lower bias as compared to ribosome-profiling. These alternative settings for the condition under MTOR inhibition are not supported by the empirical data that were obtained (**Sup. Fig. 1-2**) and does affect the size of the shifts and thus an increased bias is expected.

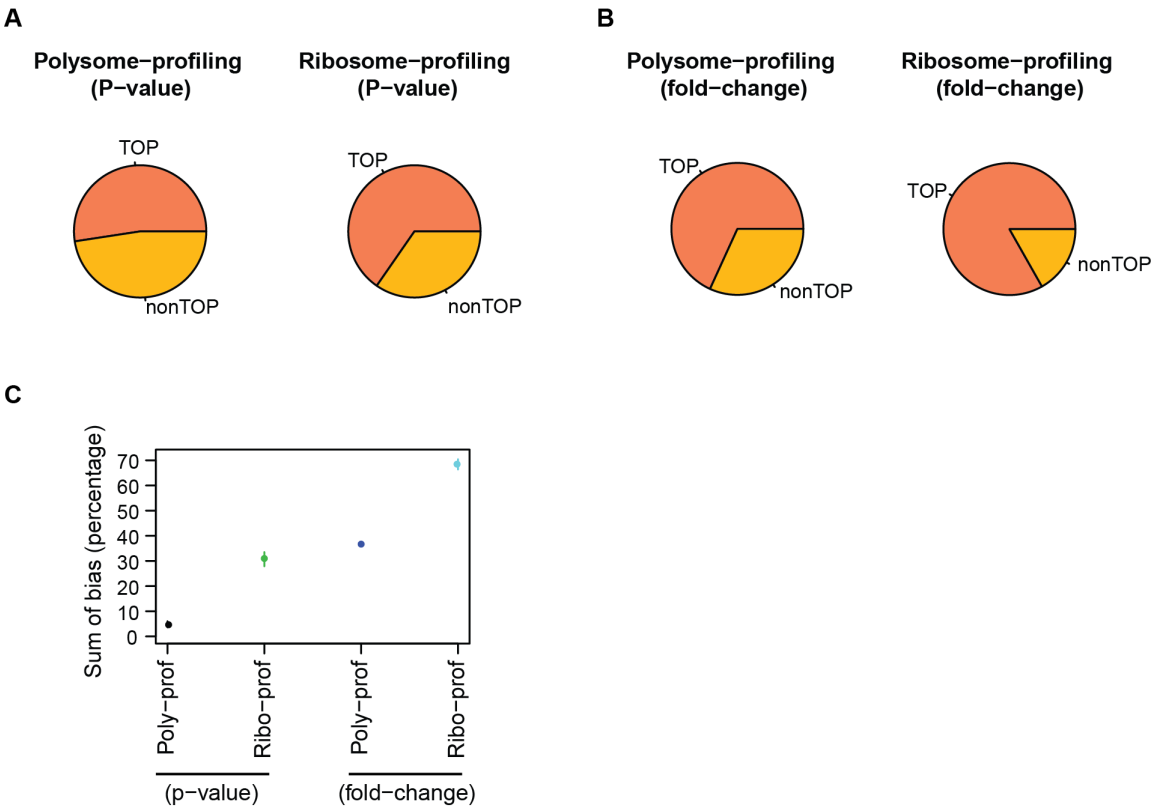

Sup. Fig. 4. Simulation of bias in identification of TOP and non-TOP mRNAs by ribosome- or polysome-profiling. The simulation was performed as in **Fig. 1D-I** except for that only those distributions resembling TOP or non-TOP mRNAs were included (as defined in **Sup. Fig. 1-2**). **(A-B)** Proportions of TOP or non-TOP mRNAs identified as differentially translated by polysome or ribosome-profiling. Genes were ranked by p-value **(A)** or fold-change **(B)**. **(C)**. Sum of bias across all shifts for each technology and analysis approach.

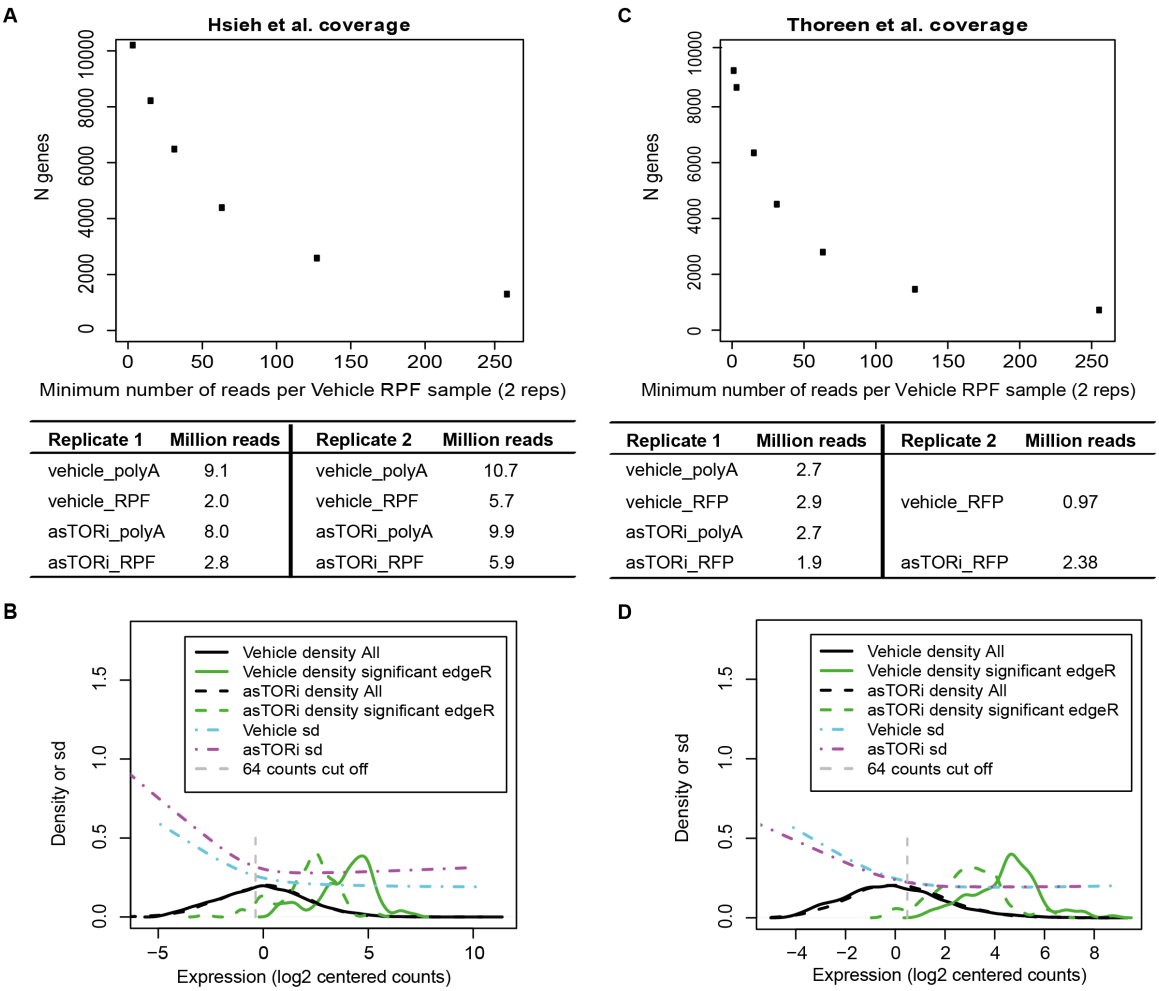

Replicate 1	Million reads	Replicate 2	Million reads
vehicle_polyA	9.1	vehicle_polyA	10.7
vehicle_RPF	2.0	vehicle_RPF	5.7
asTORi_polyA	8.0	asTORi_polyA	9.9
asTORi_RPF	2.8	asTORi_RPF	5.9

Replicate 1	Million reads	Replicate 2	Million reads
vehicle_polyA	2.7		
vehicle_RFP	2.9	vehicle_RFP	0.97
asTORi_polyA	2.7		
asTORi_RFP	1.9	asTORi_RFP	2.38

Sup. Fig. 5. Low sensitivity in ribosome-profiling studies obscures identification of the complete catalogue of MTOR-sensitive mRNAs. (A, C) The number of genes detected under different thresholds for minimum number of RNA-seq reads under the control condition (ribosome protected fragment [RPF] data; top). The number of reads mapped to protein coding genes under the indicated conditions and replicates (bottom). **(B, D)** Comparisons of RPF signals and standard deviations for all genes or differentially expressed genes (edgeR FDR<0.05) under control conditions or conditions when MTOR is inactive. A cutoff for 64 reads in the RPF control condition is indicated.

A

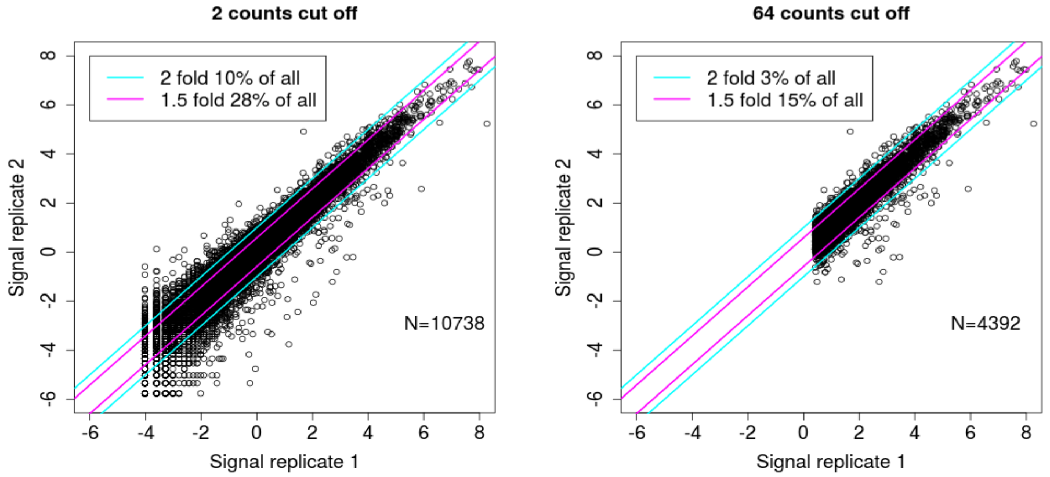
2 counts cut off
2 fold 10% of all
1.5 fold 28% of all
N=10738
Signal replicate 2
Signal replicate 1
64 counts cut off
2 fold 3% of all
1.5 fold 15% of all
N=4392
Signal replicate 2
Signal replicate 1

B

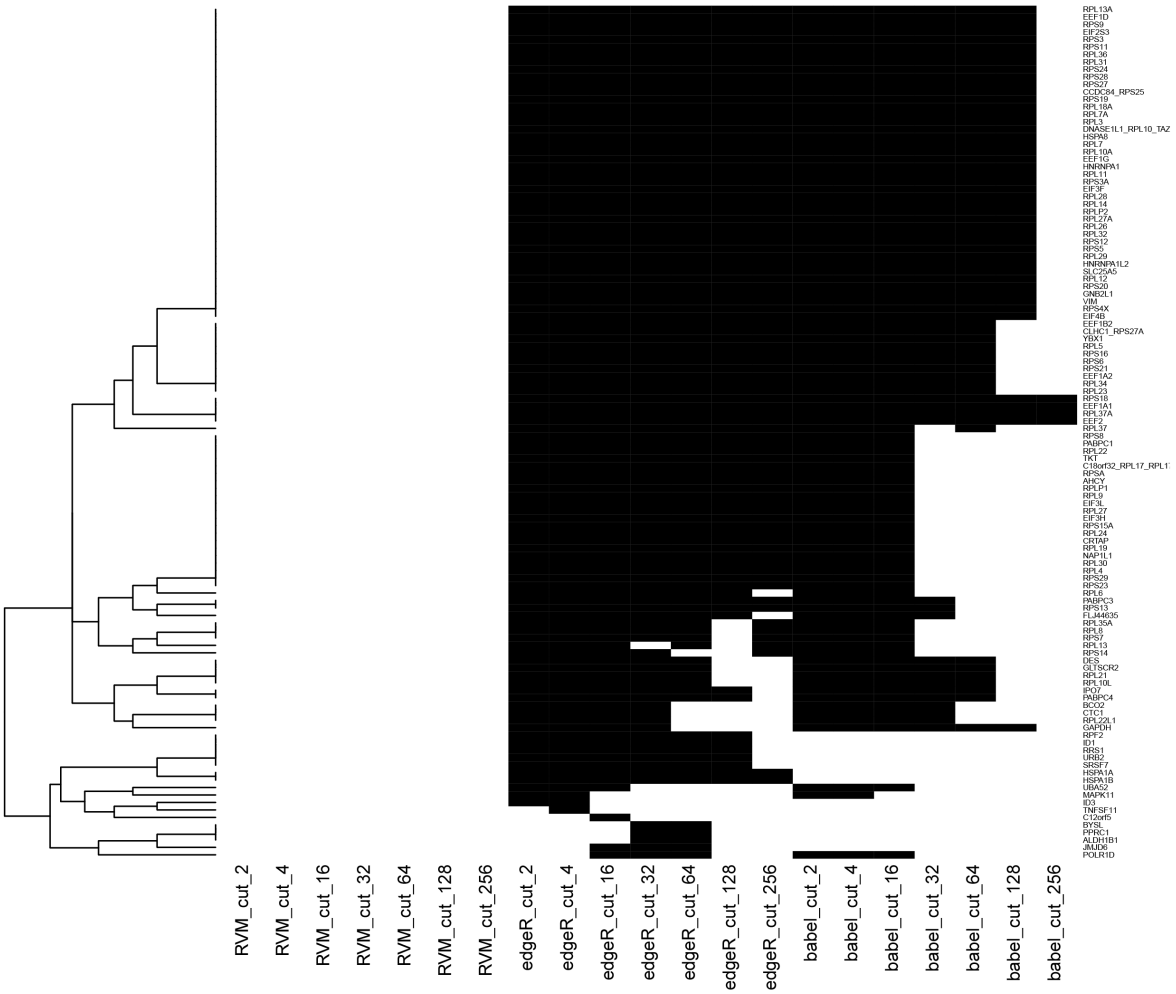
RVM_cut_2
RVM_cut_4
RVM_cut_16
RVM_cut_32
RVM_cut_64
RVM_cut_128
RVM_cut_256
edgeR_cut_2
edgeR_cut_4
edgeR_cut_16
edgeR_cut_32
edgeR_cut_64
edgeR_cut_128
edgeR_cut_256
babel_cut_2
babel_cut_4
babel_cut_16
babel_cut_32
babel_cut_64
babel_cut_128
babel_cut_256

Sup. Fig. 6. Across replicate reproducibility for ribosome-profiling and genes identified as differentially translated in the study by Hsieh et al. (A) A comparison of signals (centered log2 counts) between replicate experiments of ribosome protected fragments under the control condition for all genes with >2 counts (left) or 64 counts (right). The percentages of genes that show 2 fold or 1.5 fold differences between replicates are indicated. The total number of genes (N) is also shown. **(B)** Heatmap of genes identified as differentially expressed by RVM or edgeR or differentially translated by babel (FDR<0.05) under a range of cut offs for minimum number of reads per replicate under the control RPF condition. Black indicates that a gene was differentially expressed.

A

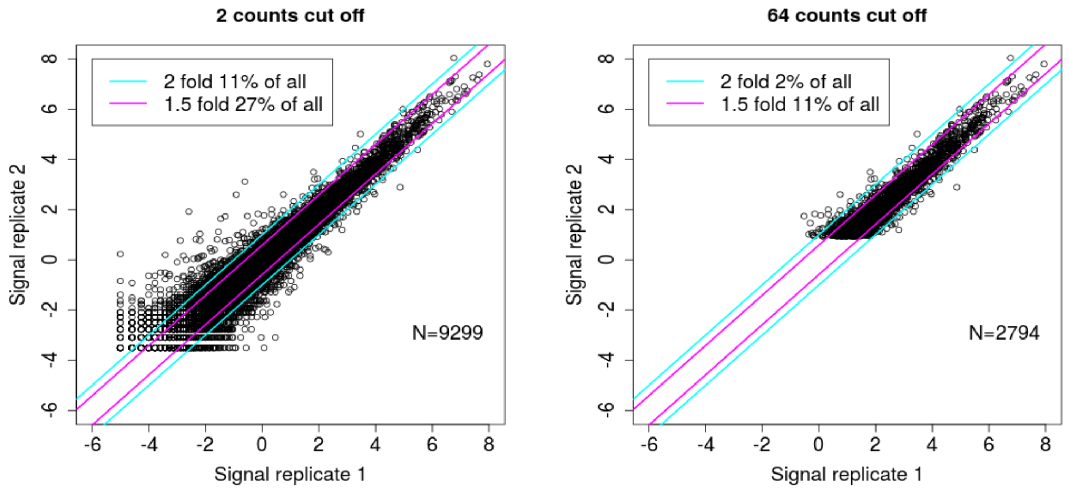
2 counts cut off
2 fold 11% of all
1.5 fold 27% of all
N=9299
Signal replicate 2
Signal replicate 1
64 counts cut off
2 fold 2% of all
1.5 fold 11% of all
N=2794
Signal replicate 2
Signal replicate 1

B

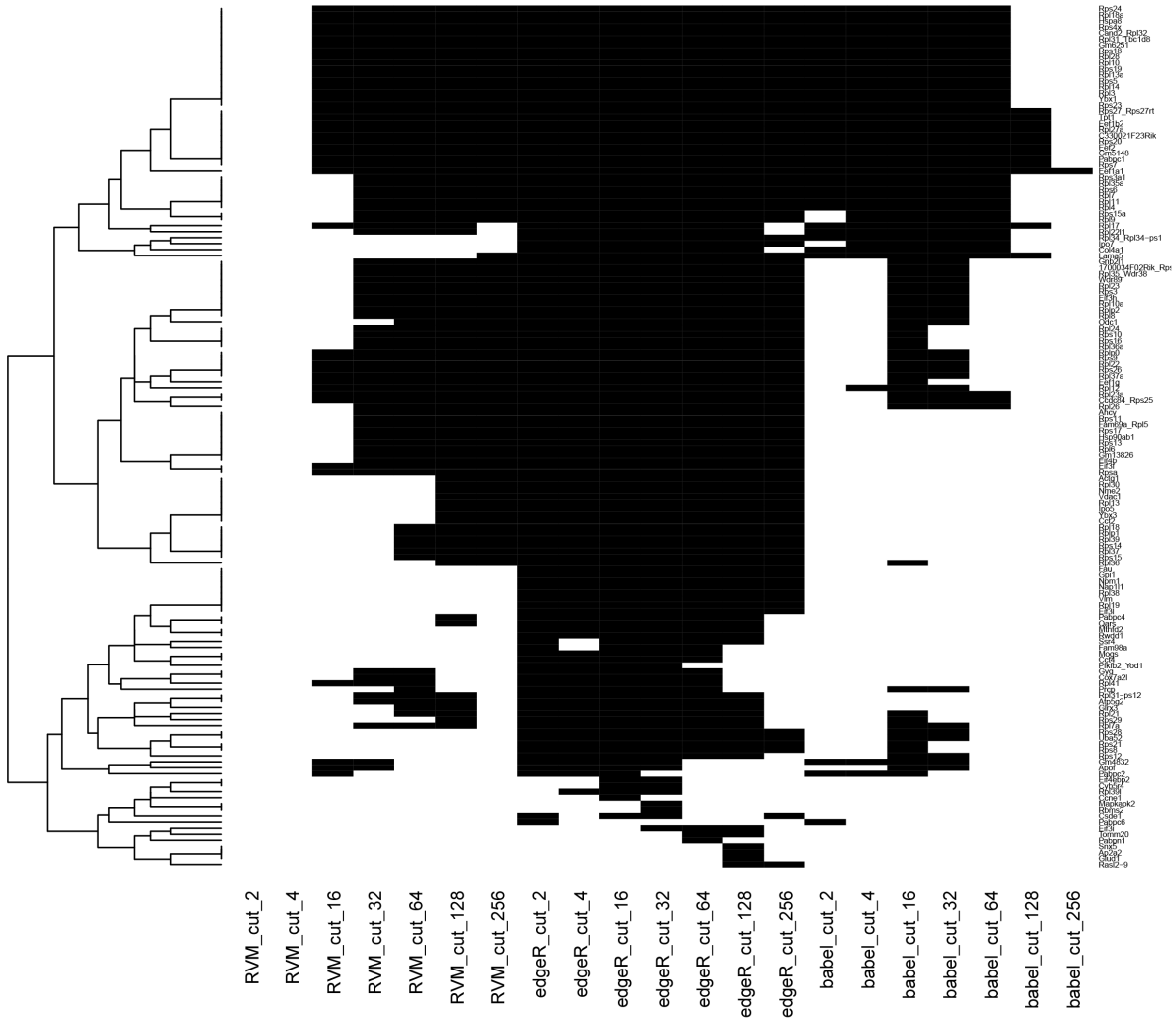
RVM_cut_2
RVM_cut_4
RVM_cut_16
RVM_cut_32
RVM_cut_64
RVM_cut_128
RVM_cut_256
edgeR_cut_2
edgeR_cut_4
edgeR_cut_16
edgeR_cut_32
edgeR_cut_64
edgeR_cut_128
edgeR_cut_256
babel_cut_2
babel_cut_4
babel_cut_16
babel_cut_32
babel_cut_64
babel_cut_128
babel_cut_256

Sup. Fig. 7. Across replicate reproducibility for ribosome-profiling and genes identified as differentially translated in the study by Thoreen et al. (A) A comparison of signals (centered log2 counts) between replicate experiments of ribosome protected fragments under the control condition for all genes with >2 counts (left) or 64 counts (right). The percentages of genes that show 2 fold or 1.5 fold differences between replicates are indicated. The total number of genes (N) is also shown. **(B)** Heatmap of genes identified as differentially expressed by RVM or edgeR or differentially translated by babel (FDR<0.05) under a range of cut offs for minimum number of reads per replicate under the control RPF condition. Black indicates that a gene was differentially expressed.

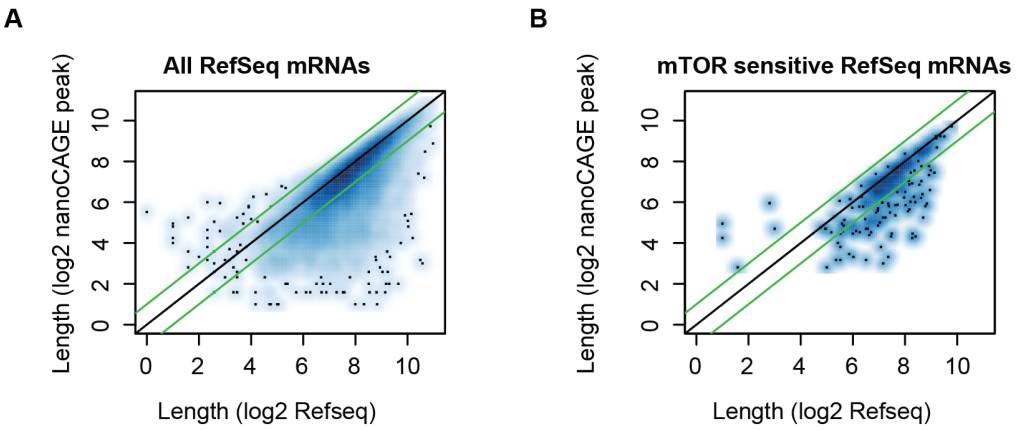

Sup. Fig. 8. Comparison of 5'UTR lengths obtained by nanoCAGE peak vs. RefSeq annotations. A comparison between 5'UTR lengths according to RefSeq and nanoCAGE peak lengths for all detected RefSeq mRNAs **(A)** and MTOR sensitive mRNAs **(B)**. Green lines indicate a 2 fold difference in 5' UTR length.

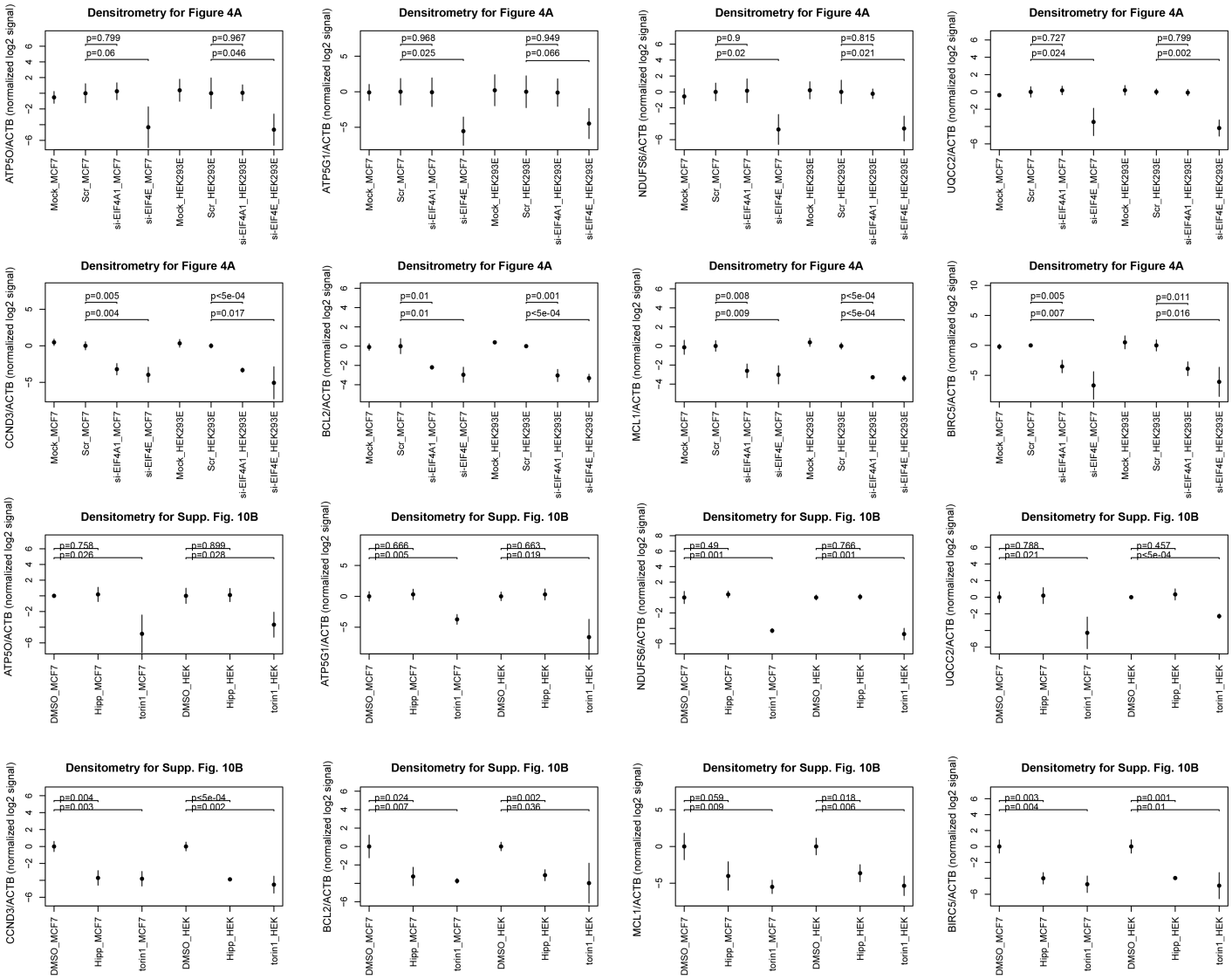

Sup. Fig. 9. Densitometry for Western blotting and related statistical analysis. Although we trust that Western blotting should be used for qualitative rather than quantitative measurements, as requested we performed densitometric analysis using ImageJ (W. S. Rasband, ImageJ; National Institutes of Health, Bethesda, MD). Shown are log2 transformed and normalized (per replicate and to mean of a selected "control" under each condition) signals for the indicated figures and protein ratios. P-values from 1-way ANOVAs are indicated. Western blotting experiments were repeated in independent triplicates.

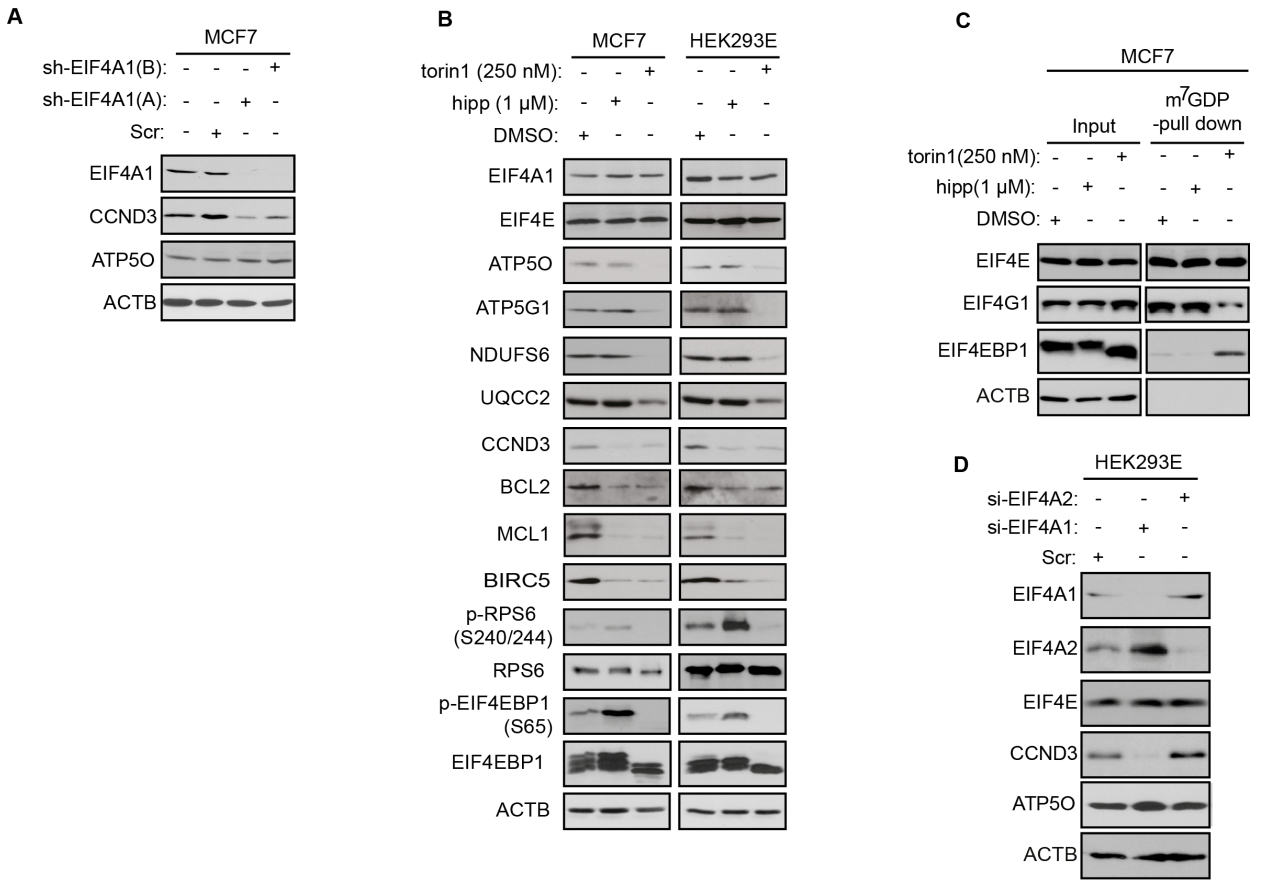

Sup. Fig. 10. Torin1 abolishes EIF4E:EIF4G1 association and decreases levels of proteins encoded by both long and short 5'UTRs MTOR-sensitive mRNAs, whereas hippuristanol downregulates proteins encoded by mRNAs harboring long, but not short 5' UTRs, and does not appear to strongly affect EIF4E:EIF4G1 binding. (A) Levels of indicated proteins in mock infected MCF7 cells or puromycin-selected MCF7 cells infected with scrambled control shRNA (Scr) or two different shRNAs targeting EIF4A1 [sh-EIF4A1(A) and sh-EIF4A1(B)] were monitored by Western blotting. (**B)** HEK293E or MCF7 cells were treated with indicated concentrations of torin1 or hippuristanol (hipp), or a vehicle (DMSO) for 6 h. Expression and the phosphorylation status of indicated proteins were determined by Western blotting. ACTB served as a loading control. Experiments were carried out in independent triplicates and quantified by densitometry (**Sup. Fig. 9**). **(C)** MCF7 cells were incubated with indicated concentrations of torin1 or hippuristanol (hipp) for 6 h and subjected to m^7GDP-pulldown. The amount of indicated proteins in m^7GDP-pulldown (25%) was determined by Western blotting. Inputs represent 10% of the extract

used in the pull-down. ACTB served as a loading control and to exclude contamination (e.g. non-specific binding of the proteins to the agarose beads) in m^7GDP-pulldown material. **(D)** HEK293E cells were transfected with scrambled control (Scr), EIF4A1 (si-EIF4A1), or EIF4A2 (si-EIF4A2) siRNA. Levels of indicated proteins were monitored 48 h post-transfection by Western blotting. ACTB served as a loading control.

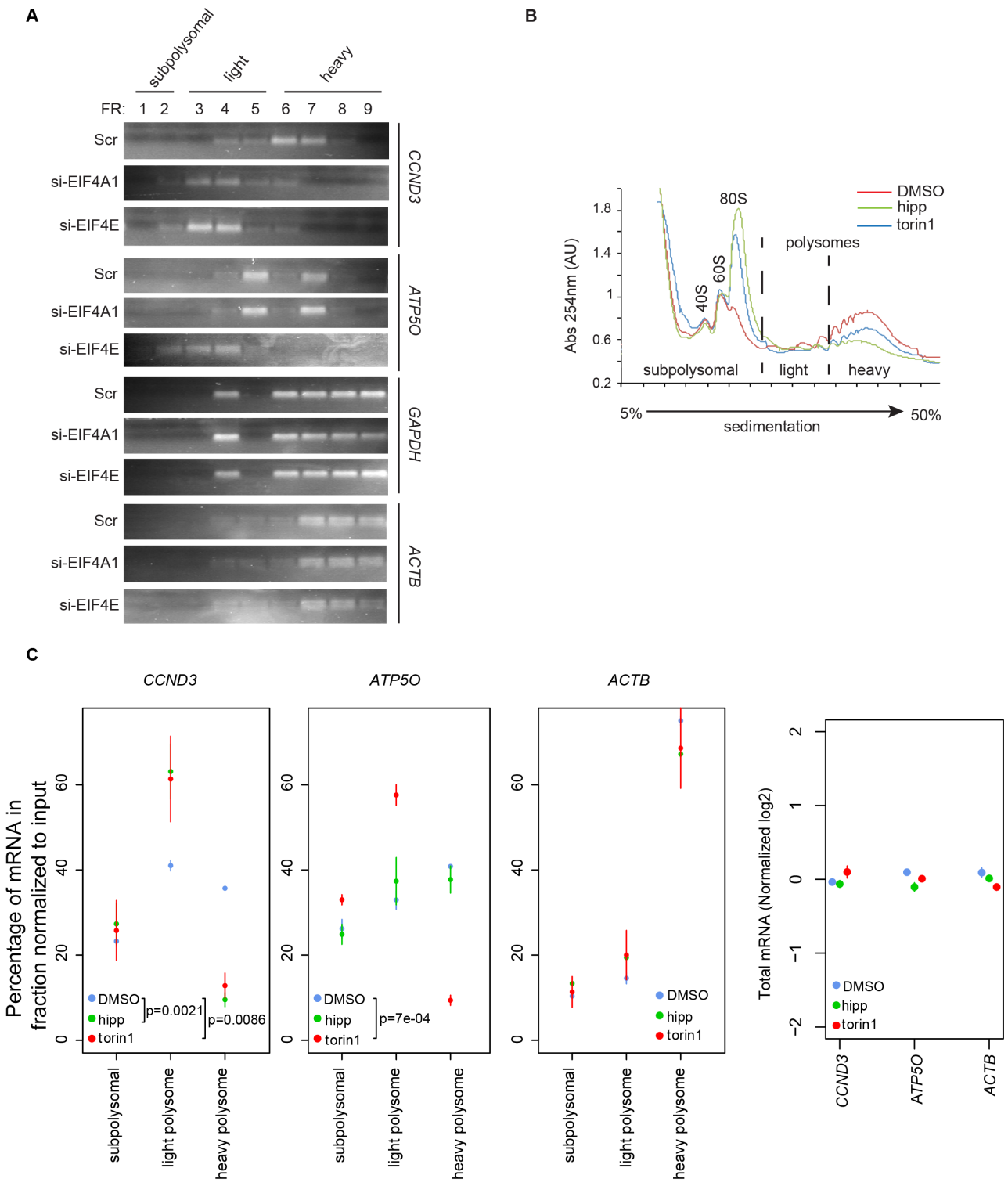

Gandin, Masvidal, Hulea et al Supplementary Fig. 11

Sup. Fig. 11. EIF4A1 inhibition and/or depletion results in selective suppression of translation of a model MTOR-sensitive mRNA with long (*CCND3*), but not short 5' UTR (*ATP5O*). (A) Amounts of indicated mRNAs in individual sucrose fractions obtained as described in **Fig. 4C-D** were monitored by RT-sqPCR. **(B)** Sub-polyosmal, light polysome and heavy polysome fractions were obtained from cytosolic extracts from MCF7 cells treated with torin1 (250 nM), hippuristanol (hipp; 1 μM) or a vehicle (DMSO) for 2 h by ultracentrifugation on 5-50% sucrose gradients. Positions of 40S and 60S ribosomal subunits, monosome (80S) and polysomes are indicated in UV absorbance at 254 nm (Abs 254 nm) spectra. (**C**) Amount of indicated mRNAs in sub-polyosmal, light polysome and heavy polysome was determined by RT-sqPCR. Data are expressed as a mean percentage of a given mRNA in each fraction. Bars represent SD values. P-values from 1-way ANOVAs for heavy polysomes are indicated. Total levels of indicated mRNAs isolated from cells described in **(B)** were determined by RT-qPCR. Data were log2 transformed and normalized to those obtained for ACTB, and to the mean expression per gene. RT-qPCR experiments were carried out in independent duplicates, whereby each replicate consisted of technical triplicate.

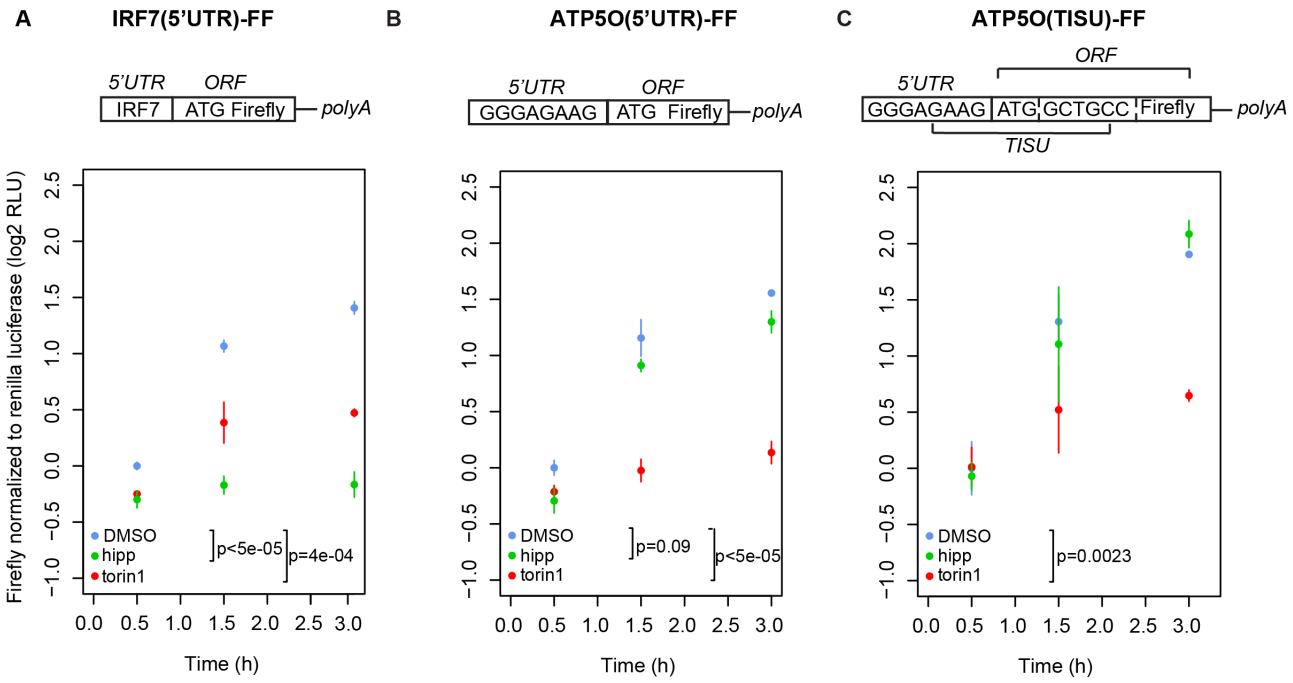

Sup. Fig. 12. Translation of reporter mRNAs harboring short 5' UTRs is sensitive to torin1, but not hippuristanol. HEK293E cells were transfected with firefly (FF) reporters harboring IRF7 5' UTR [IRF7(5'UTR)-FF] **(A)** ATP5O 5'UTR with a proximal portion of TISU element before the initiation codon [ATP5O(5'UTR)-FF] **(B)** or ATP5O 5'UTR with a full TISU element [ATP5O(TISU)-FF] **(C).** 48 h post-transfection cells were treated with 250 nM torin1, 1 μM hippuristanol (hipp) or a vehicle (DMSO) and the luminescence was measured at the indicated time points. Data are depicted as mean firefly luminescence normalized to renilla luminescence (see **Suppl. Fig. 13**). Each experiment was performed in independent triplicates each consisting of 3 technical replicates. Data were log2 transformed normalized per replicate and to the mean of DMSO at 0.5 h; and are shown as a mean +/- SD. RLU, relative light units. Treatment p-values from 2-way ANOVAs are indicated.

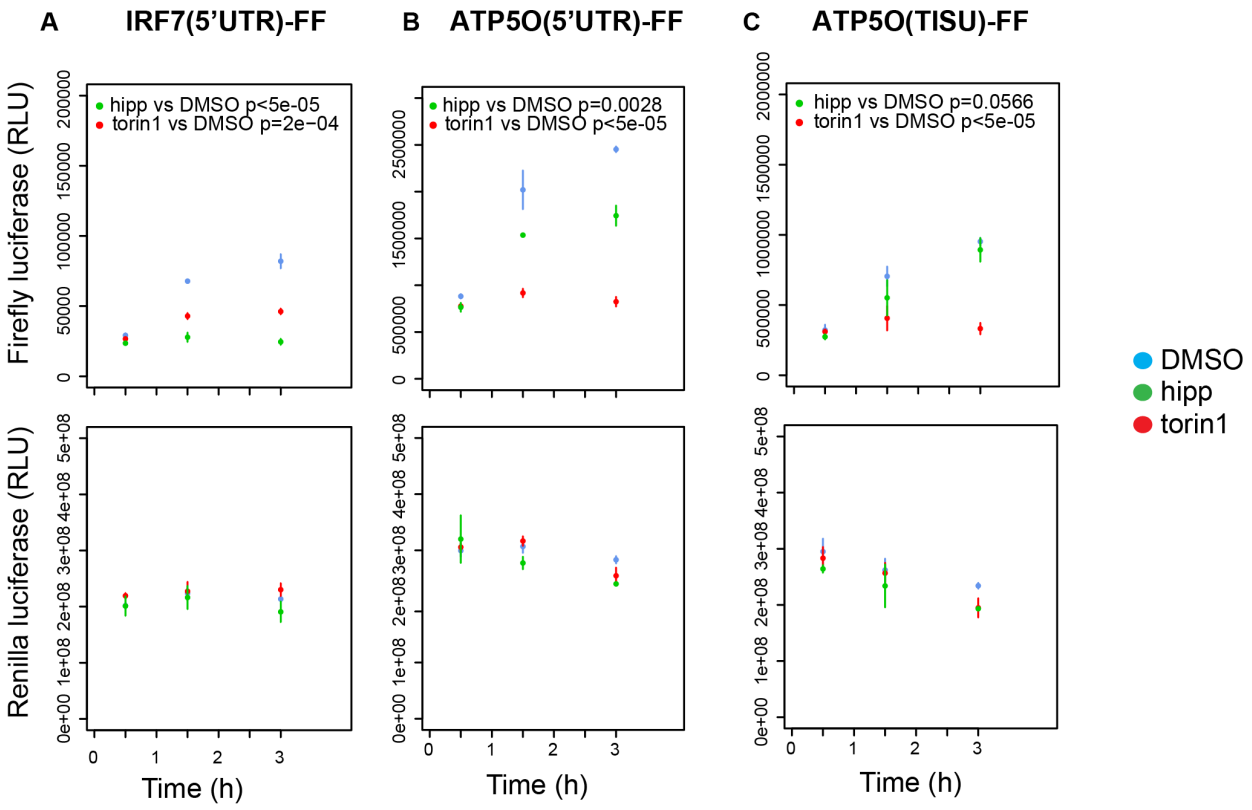
A
IRF7(5'UTR)-FF
B
ATP5O(5'UTR)-FF
C
ATP5O(TISU)-FF
hipp vs DMSO p<5e-05
torin1 vs DMSO p=2e−04
hipp vs DMSO p=0.0028
torin1 vs DMSO p<5e-05
hipp vs DMSO p=0.0566
torin1 vs DMSO p<5e-05
Firefly luciferase (RLU)
Renilla luciferase (RLU)
Time (h)
DMSO
hipp
torin1

Sup. Fig 13

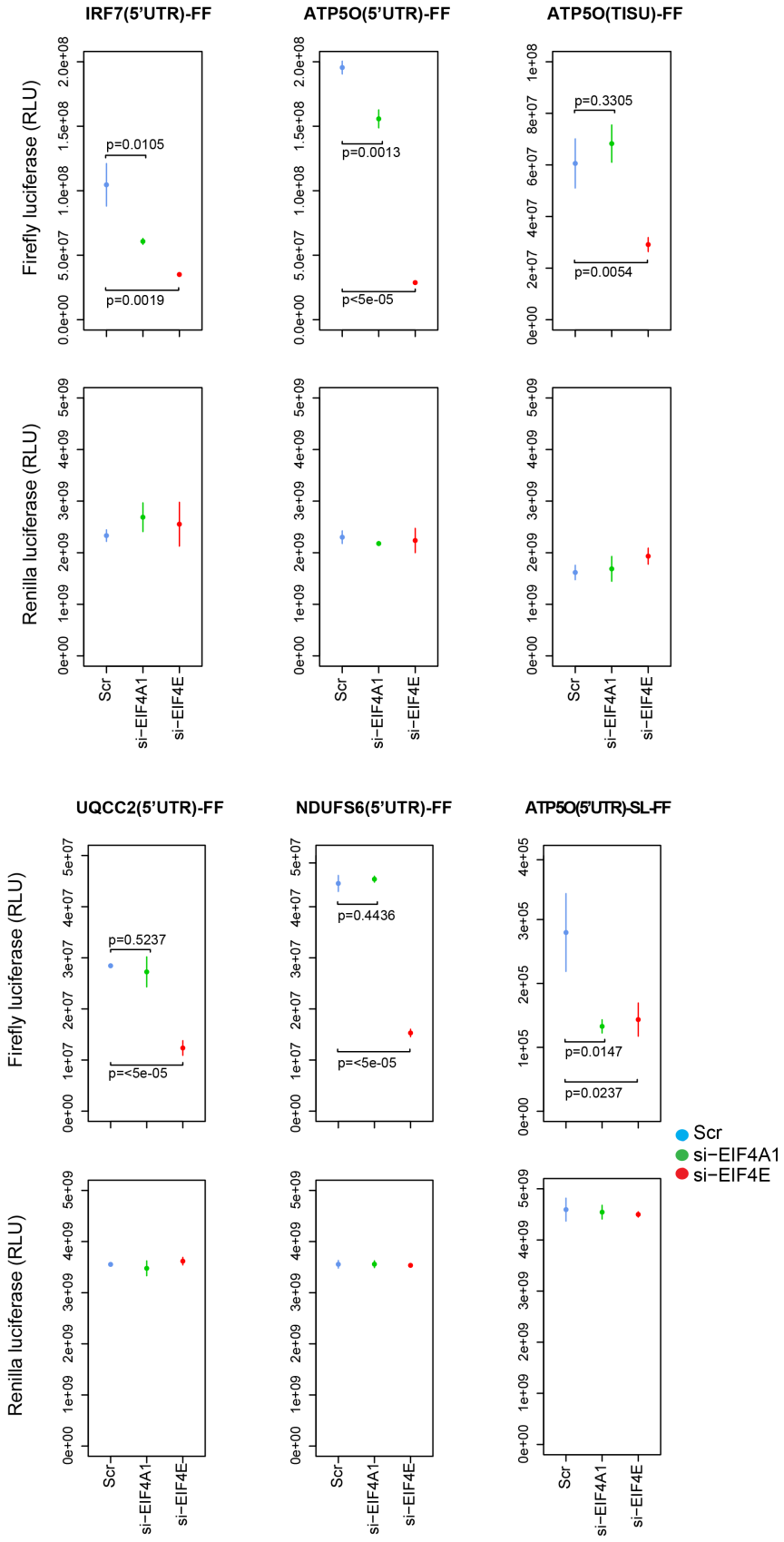
IRF7(5'UTR)-FF
ATP5O(5'UTR)-FF
ATP5O(TISU)-FF
UQCC2(5'UTR)-FF
NDUFS6(5'UTR)-FF
ATP5O(5'UTR)-SL-FF
Firefly luciferase (RLU)
Renilla luciferase (RLU)
p=0.0105
p=0.0019
p=0.0013
p<5e-05
p=0.3305
p=0.0054
p=0.5237
p=<5e-05
p=0.4436
p=<5e-05
p=0.0147
p=0.0237
Scr
si-EIF4A1
si-EIF4E

Sup. Fig. 13-14. Separate Firefly luciferase (FL) and Renilla luciferase (RL) measurements for ratios presented in Fig. 5 and Sup. Fig. 12, respectively. Data are depicted as relative light units (RLU) for the firefly (left panels) and renilla (right panels) luciferase, respectively. Luminescence was monitored 48 h post-transfection. Each experiment was performed in independent triplicate each consisting of 3 technical replicates. Data are shown as mean +/- SD. Treatment p-values from 2-way (**Sup. Fig. 13**) or 1-way (**Sup. Fig. 12**) ANOVAs are shown.

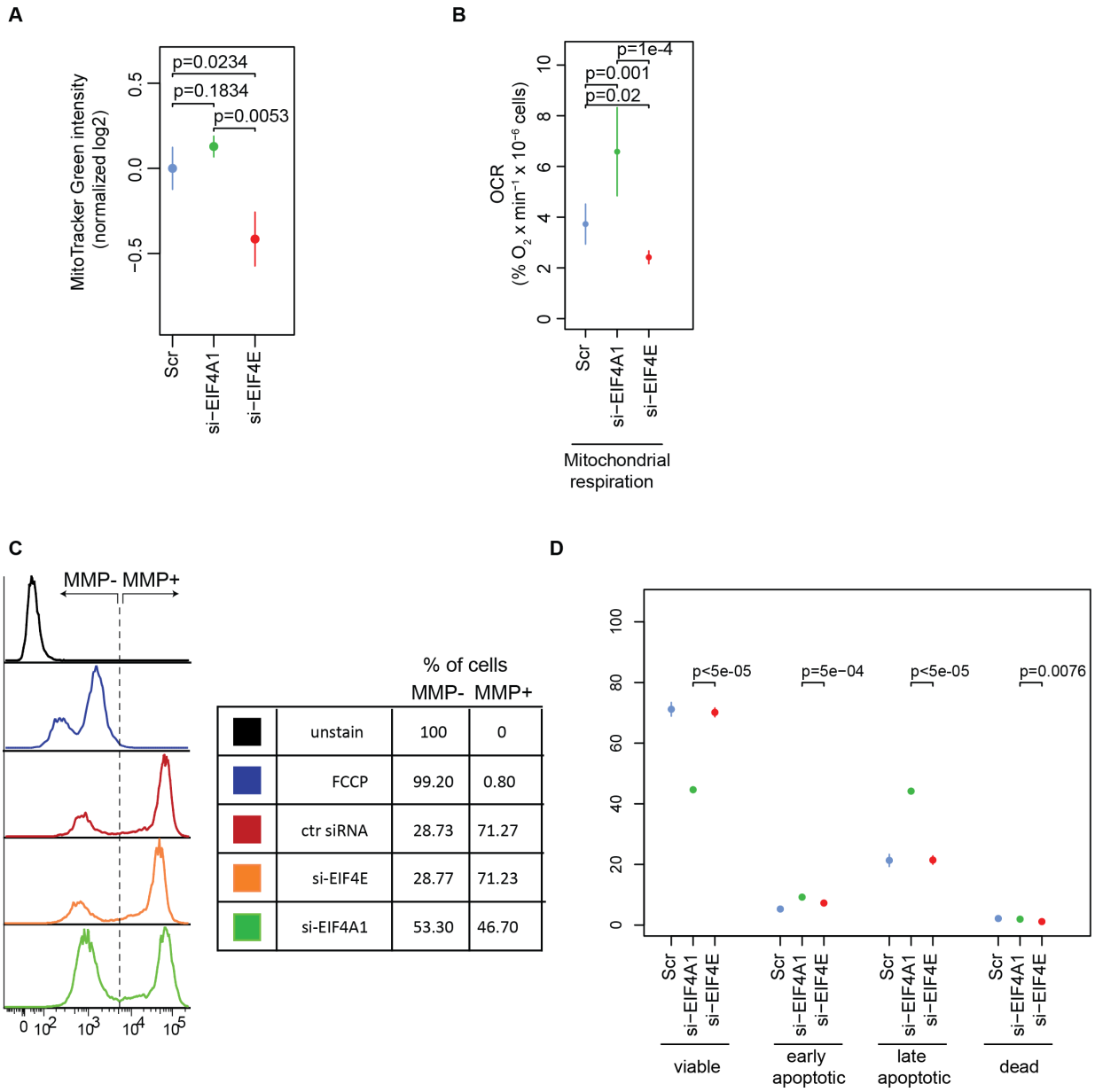

Sup. Fig. 15. Depletion of EIF4**E, but not** EIF4**A1, reduces mitochondrial number and respiration, whereas downregulation of** EIF4**A1, but not** EIF4**E, sensitizes cells to starvation-induced apoptosis. (A)** HEK293E cells were transfected with control (Scr), EIF4E or EIF4A1 siRNA. After 48 h, mitochondrial mass was estimated by monitoring mean fluorescence intensity of MitoTracker Green using flow cytometry. Data were log2 transformed, normalized per replicate and to the mean of the control (Scr), and are shown as means +/- SD from 3 independent experiments. P-values from 1-way ANOVAs are indicated. **(B)** Mitochondrial respiration in cells and under conditions described in **(A)** was measured

using a Clark electrode and presented as oxygen consumption rate (OCR). Data are shown as means from 4 independent experiments +/- SD. P-values from 1-way ANOVAs calculated after log2 transformation and normalization per replicate and to control (DMSO) are indicated. **(C)** Cells were transfected as described in **(A)** and after 72 h, cultivated in FBS and glucose-free media for an additional 18 h to induce apoptosis. Mitochondrial membrane polarization (MMP) was analyzed by monitoring TMRE fluorescence intensity by flow cytometry. As a control, cells were treated for 10 min with FCCP (20 μM) to induce mitochondrial membrane depolarization. Left panel: The flow cytometry histogram profiles of unstained (control; black), and TMRE stained cells treated with FCCP (blue), control siRNA (red), EIF4E siRNA (orange) or EIF4A1 siRNA (green). Cells harboring depolarized mitochondria (MMP-) were defined as those with TMRE signal equal of less to TMRE signal observed in FCCP-treated cells. Right panel: Mean percentage (3 independent replicates) of MMP- and MMP+ cells out of total cells. **(D)** Apoptosis in HEK293E cells described in **(C)** was monitored using a FITC-Annexin V – PI staining and analyzed by flow cytometry. The fractions (%) of viable (Annexin V-/ PI-), early apoptotic (Annexin V+/ PI-), late apoptotic (Annexin V+/PI low), and dead (Annexin V+/ PI high) cells are shown relative to the total cell population. Results represent means +/- SD of 3 independent experiments. P-values from 1-way ANOVAs are indicated.

Supplementary References:

Babendure JR, Babendure JL, Ding JH, Tsien RY. 2006. Control of mammalian translation by mRNA structure near caps. *RNA* **12**(5): 851-861.

Benjamini Y, Hochberg Y. 1995. Controlling the False Discovery Rate: A Practical and Powerful Approach to Multiple Testing. *Journal of the Royal Statistical Society Series B (Methodological)* **57**(1): 289-300.

Colina R, Costa-Mattioli M, Dowling RJ, Jaramillo M, Tai LH, Breitbach CJ, Martineau Y, Larsson O, Rong L, Svitkin YV et al. 2008. Translational control of the innate immune response through IRF-7. *Nature* **452**(7185): 323-328.

Dowling RJ, Topisirovic I, Alain T, Bidinosti M, Fonseca BD, Petroulakis E, Wang X, Larsson O, Selvaraj A, Liu Y et al. 2010. mTORC1-mediated cell proliferation, but not cell growth, controlled by the 4E-BPs. *Science* **328**(5982): 1172-1176.

Edery I, Altmann M, Sonenberg N. 1988. High-level synthesis in Escherichia coli of functional cap-binding eukaryotic initiation factor eIF-4E and affinity purification using a simplified cap-analog resin. *Gene* **74**(2): 517-525.

Elfakess R, Dikstein R. 2008. A translation initiation element specific to mRNAs with very short 5'UTR that also regulates transcription. *PLoS One* **3**(8): e3094.

Elfakess R, Sinvani H, Haimov O, Svitkin Y, Sonenberg N, Dikstein R. 2011. Unique translation initiation of mRNAs-containing TISU element. *Nucleic Acids Res* **39**(17): 7598-7609.

Gandin V, Sikstrom K, Alain T, Morita M, McLaughlan S, Larsson O, Topisirovic I. 2014. Polysome fractionation and analysis of mammalian translatomes on a genome-wide scale. *Journal of visualized experiments : JoVE*(87).

Hsieh AC, Liu Y, Edlind MP, Ingolia NT, Janes MR, Sher A, Shi EY, Stumpf CR, Christensen C, Bonham MJ et al. 2012. The translational landscape of mTOR signalling steers cancer initiation and metastasis. *Nature* **485**(7396): 55-61.

Kim D, Langmead B, Salzberg SL. 2015. HISAT: a fast spliced aligner with low memory requirements. *Nature methods* **12**(4): 357-360.

Kim JE, Chen J. 2000. Cytoplasmic-nuclear shuttling of FKBP12-rapamycin-associated protein is involved in rapamycin-sensitive signaling and translation initiation. *Proc Natl Acad Sci U S A* **97**(26): 14340-14345.

Langmead B, Trapnell C, Pop M, Salzberg SL. 2009. Ultrafast and memory-efficient alignment of short DNA sequences to the human genome. *Genome Biol* **10**(3): R25.

Larsson O, Morita M, Topisirovic I, Alain T, Blouin MJ, Pollak M, Sonenberg N. 2012. Distinct perturbation of the translatome by the antidiabetic drug metformin. *Proc Natl Acad Sci U S A* **109**(23): 8977-8982.

Lassmann T. 2015. TagDust2: a generic method to extract reads from sequencing data. *BMC Bioinformatics* **16**: 24.

Luo W, Friedman MS, Shedden K, Hankenson KD, Woolf PJ. 2009. GAGE: generally applicable gene set enrichment for pathway analysis. *BMC Bioinformatics* **10**: 161.

Olshen AB, Hsieh AC, Stumpf CR, Olshen RA, Ruggero D, Taylor BS. 2013. Assessing gene-level translational control from ribosome profiling. *Bioinformatics* **29**(23): 2995-3002.

Ramskold D, Wang ET, Burge CB, Sandberg R. 2009. An abundance of ubiquitously expressed genes revealed by tissue transcriptome sequence data. *PLoS Comput Biol* **5**(12): e1000598.

Robinson MD, McCarthy DJ, Smyth GK. 2010. edgeR: a Bioconductor package for differential expression analysis of digital gene expression data. *Bioinformatics* **26**(1): 139-140.

Salimullah M, Sakai M, Plessy C, Carninci P. 2011. NanoCAGE: a high-resolution technique to discover and interrogate cell transcriptomes. *Cold Spring Harb Protoc* **2011**(1): pdb prot5559.

Tang DT, Plessy C, Salimullah M, Suzuki AM, Calligaris R, Gustincich S, Carninci P. 2013. Suppression of artifacts and barcode bias in high-throughput transcriptome analyses utilizing template switching. *Nucleic Acids Res* **41**(3): e44.

Thoreen CC, Chantranupong L, Keys HR, Wang T, Gray NS, Sabatini DM. 2012. A unifying model for mTORC1-mediated regulation of mRNA translation. *Nature* **485**(7396): 109-113.

Topisirovic I, Siddiqui N, Orolicki S, Skrabanek LA, Tremblay M, Hoang T, Borden KL. 2009. Stability of eukaryotic translation initiation factor 4E mRNA is regulated by HuR, and this activity is dysregulated in cancer. *Mol Cell Biol* **29**(5): 1152-1162.

Wright GW, Simon RM. 2003. A random variance model for detection of differential gene expression in small microarray experiments. *Bioinformatics* **19**(18): 2448-2455.